Deep Inelastic ν Scattering: Recent Results and Future

D.Naples
University of Pittsburgh

NuInt 2007
Fermilab
June 3, 2007

Outline

- Overview of Neutrino DIS
- Recent Results
  - NuTeV
  - Chorus
  - Nomad ***WIP***

  } *High energy range 10-300 GeV*
- Future
  - Minos ***WIP***
  - Minerva

  } *Low energy range 5-50 GeV*

CC Neutrino Deep Inelastic Scattering

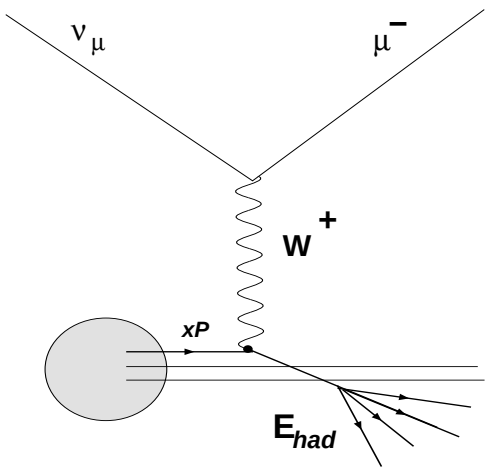

Lorentz-invariant quantities in terms of measured $E_\mu,\ \theta_\mu,\ E_{had}$:

$$\begin{cases} Q^2 = 4(E_\mu + E_{had})E_\mu sin^2\frac{\theta_\mu}{2} & \longrightarrow \text{Squared 4-momentum transfer} \\ x = \frac{Q^2}{2ME_{had}} & \longrightarrow \text{Fractional struck quark momentum} \\ y = \frac{E_{had}}{E_\mu + E_{had}} & \longrightarrow \text{Inelasticity} \\ W^2 = M^2 + 2ME_{\mathrm{HAD}} - Q^2 & \longrightarrow \text{Squared invariant final state mass} \\ \nu = E_{had} & \longrightarrow \text{Energy transfered to hadronic system} \end{cases}$$

Neutrino Scattering Cross-Section:

$$\frac{d^2\sigma^{\nu(\overline{\nu})}}{dxdy} = \frac{G_F^2 M E_\nu}{\pi(1+\frac{Q^2}{M_W^2})^2}\left[\left(1 - y - \frac{Mxy}{2E_\nu}\right)F_2^{\nu(\overline{\nu})} + \frac{y^2}{2}2xF_1^{\nu(\overline{\nu})} \pm y(1-\frac{y}{2})xF_3^{\nu(\overline{\nu})}\right]$$

Structure functions in the parton model:

- $2xF_1^{\nu(\overline{\nu})}(x,Q^2) = \Sigma\left[xq^{\nu(\overline{\nu})} + \overline{x}q^{\nu(\overline{\nu})}\right]$
- $F_2^{\nu(\overline{\nu})}(x,Q^2) = \Sigma\left[xq^{\nu(\overline{\nu})} + x\overline{q}^{\nu(\overline{\nu})} + 2xk^{\nu(\overline{\nu})}\right]$
- $xF_3^{\nu(\overline{\nu})}(x,Q^2) = \Sigma\left[xq^{\nu(\overline{\nu})} - x\overline{q}^{\nu(\overline{\nu})}\right]$

$$2xF_1(x,Q^2) = \frac{1+(2Mx/Q)^2}{1+R(x,Q^2)}F_2(x,Q^2)$$

Neutrinos as Probes

Challenges

- ν Flux spectrum is difficult to predict/measure.
- Statistical precision
  - Require *highly intense* ν beams.
  - Massive Detectors $\Rightarrow$ *Nuclear Effects*

F_2 $\longrightarrow$ measured precisely by charged-lepton DIS.

xF_3 $\longrightarrow$ uniquely determined by neutrino DIS

- Sensitive to valence quark distributions.
- Non-singlet QCD evolution, theoretically more robust.
- $\Delta xF_3 \Rightarrow$ sensitive to strange and charm pdfs.
  $x(F_3^{\nu} - F_3^{\overline{\nu}}) = 4x(s - c)$

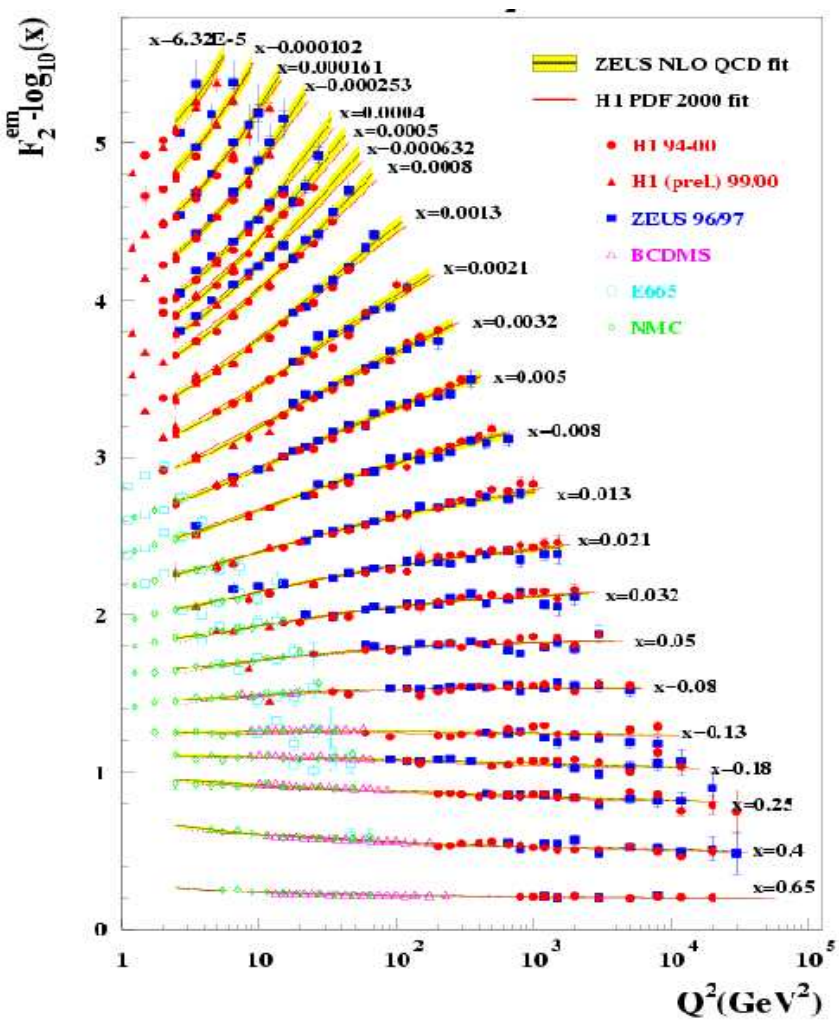

High Energy Range:

NuTeV, Chorus, Nomad

NuTeV

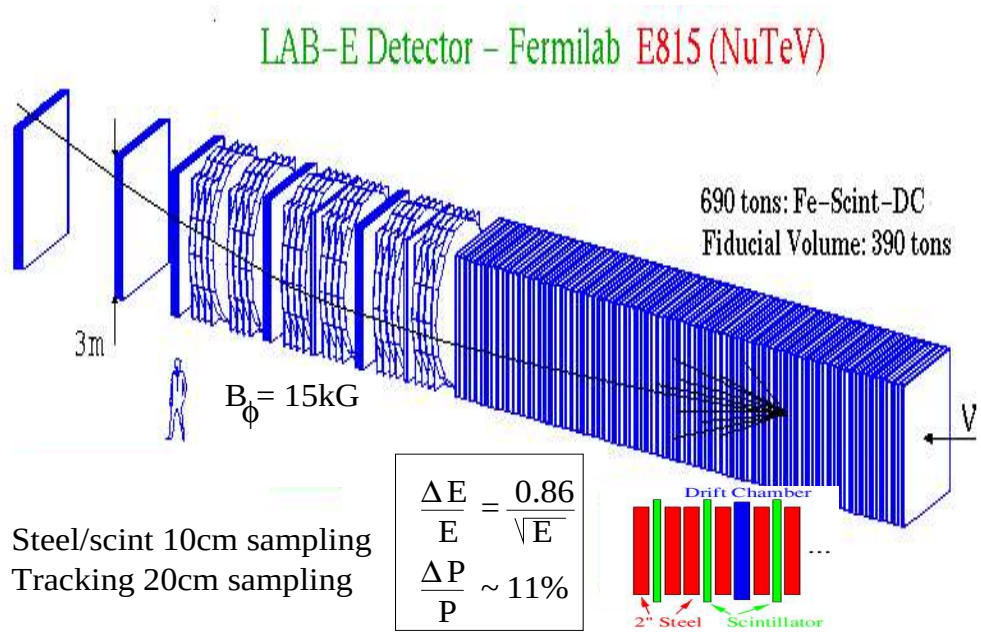

- Data taking: 1996-97 FNAL fixed target.
- Many physics topics $\Rightarrow$ Main motivation: precise meas. of $\sin^2\theta_W$. [PRL 88, 091802 (2002)]
- Iron Calorimeter + Muon Spectrometer
- SF events: 8.6×10^5 ν and 2.3×10^5 $\overline{\nu}$
  $< E_\nu > \sim 120$ GeV, $< Q^2 > \sim 25$ GeV^2

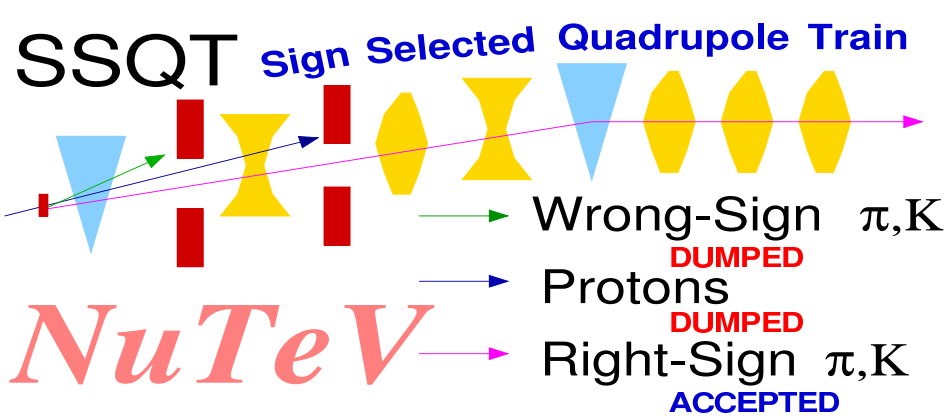

- Sign-selected: **Separate high-purity ν or $\overline{\nu}$**
  - ν mode 3×10^{-4} $\overline{\nu}$
  - $\overline{\nu}$ mode 4×10^{-3} ν
- Tags leading muon in CC interactions
  - Toroid polarity always focusing 'right' sign μ.
  - Lead $\mu \rightarrow$ Dimuon event sample

Continuous Calibration

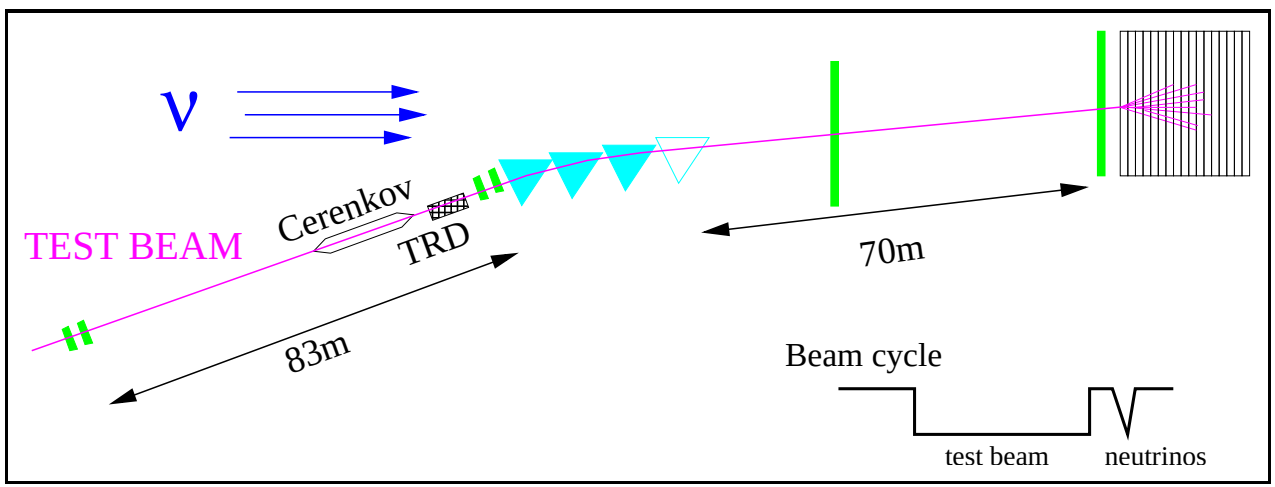

Precise in-situ calibration of NuTeV Detector:

- Alternate every cycle with Neutrino beam.
- Hadrons, muons, electrons (4.5–190GeV)
- Ability to map response.
- IMPROVED: Calibration of Energy Scale.
  - Hadrons: $\frac{\Delta E_{\rm HAD}}{E_{\rm HAD}} = 0.43\%$
  - Muons: $\frac{\Delta E_{\mu}}{E_{\mu}} = 0.7\%$

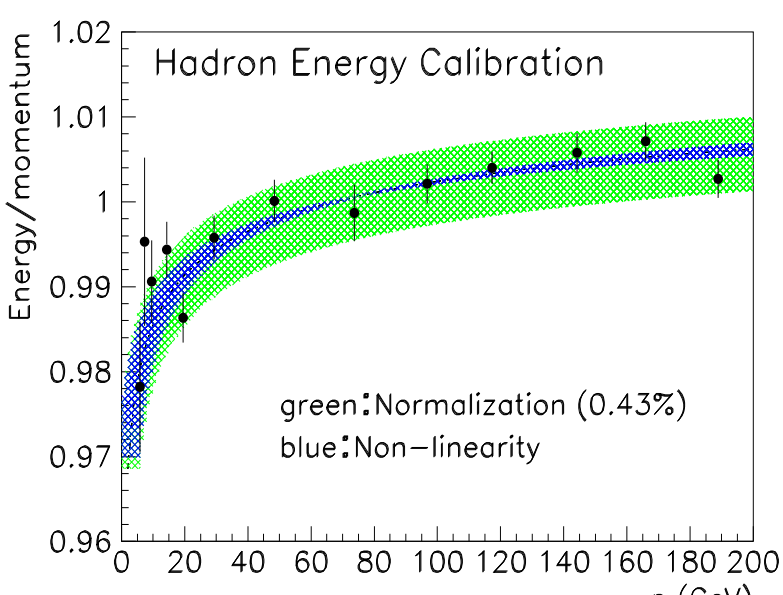

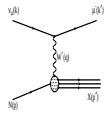

Cross Section Extraction

Differential Cross Section in terms of flux and number of events: $\frac{d^2\sigma_{ijk}^{\nu(\overline{\nu})}}{dxdy} \propto \frac{1}{\Phi(E_i^\nu)} \frac{\Delta N_{ijk}^{\nu(\overline{\nu})}}{\Delta x_j \Delta y_k}$

- **Data:**
  - CC Event Sample: toroid analyzed muon
    - ⋆ Containment and good muon track
    - ⋆ $E_\mu > 15\ GeV$, $E_\nu \in (30\ ,\ 350)\ GeV$,
  - Flux Sample:
    - ⋆ Low ν CC events ($E_{had} < 20\ GeV$)
  - Cross Section Sample:
    - ⋆ $E_{had} > 10\ GeV$,$Q^2 > 1\ GeV^2$
- **Monte Carlo:**
  - Used for acceptance and smearing corrections
  - Cross-Section Model
    - ⋆ LO QCD inspired parametrization: fi t to data : [A.Buras, K.Gaemers; Nucl.Phys.B132,249(1978)
    - ⋆ Data with lower Q^2 at high-x ($x > 0.4$) included in fi t to constrain higher-twist. (SLAC,NMC,BCDMS)
    - ⋆ for $Q^2 < 1.35\ GeV^2$ use GRV Q^2 evolution
  - Detector model:
    - ⋆ E_μ and E_{had} resolution functions parametrized using test beam
    - ⋆ θ_μ parametrized using GEANT hit level MC

- [Phys. Rev. D 74, 012008 (2006)]

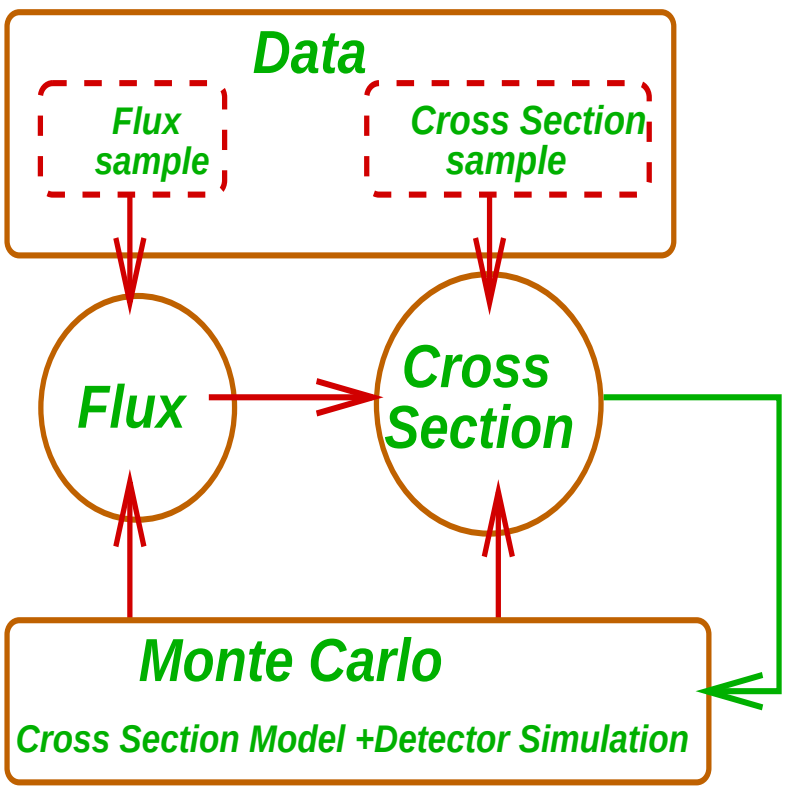

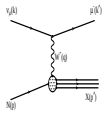

Relative Flux Extraction

"Low ν method": Integrate data at low ν (<20 GeV)

- Integrate diff. cross section over x at fi xed ν:

$$\frac{d\sigma}{d\nu} = A(1 + \frac{B}{A}\underbrace{\frac{\nu}{E_\nu}}_{small} - \frac{C}{A}\underbrace{\frac{\nu^2}{2E_\nu^2}}_{small})^{\nu\to 0}\longrightarrow A$$

$$\begin{cases} A = \frac{G_F^2 M}{\pi}\int F_2(x,Q^2)dx \\ B = -\frac{G_F^2 M}{\pi}\int [F_2(x,Q^2) \mp xF_3(x,Q^2)]dx \\ C = B - \frac{G_F^2 M}{\pi}\int F_2(x,Q^2)\left(\frac{1+\frac{2Mx}{\nu}}{1+R(x,Q^2)} - \frac{Mx}{\nu} - 1\right)dx \end{cases}$$

- $\frac{\nu}{E}$ and $(\frac{\nu}{E})^2$ terms small at low ν and high E.
- Cross section constant, indep. of E_ν
- $\Phi(E) \propto N(E, \nu < \nu_o)$

$$\Phi(E_\nu) = \int_0^{\nu_0} \frac{\frac{dN}{d\nu}}{1 + \frac{B}{A}\frac{\nu}{E_\nu} - \frac{C}{A}\frac{\nu^2}{2E_\nu^2}} d\nu$$

- Fit to $\frac{dN}{d\nu}$ data determines $\frac{B}{A}$, $\frac{C}{A}$

- Flux normalized using total neutrino cross section world average (30-200 GeV):
  $\frac{\sigma^\nu}{E} = 0.677 \pm 0.014 \times 10^{-38}\,\frac{cm^2}{GeV}$
- Test of Flux extraction:

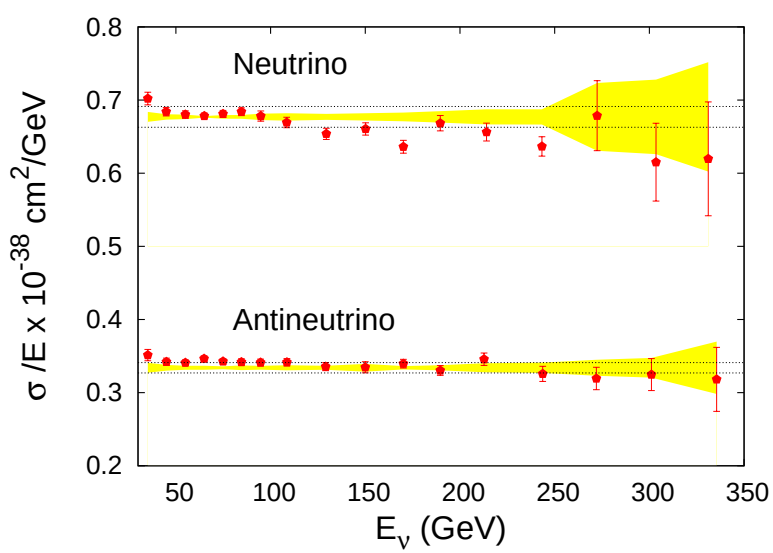

- $\frac{\sigma^\nu}{E_\nu}$ is flat as function of E_ν
- $\frac{\sigma^{\overline{\nu}}}{\sigma^\nu}$ agrees with world average

Modeling of Data

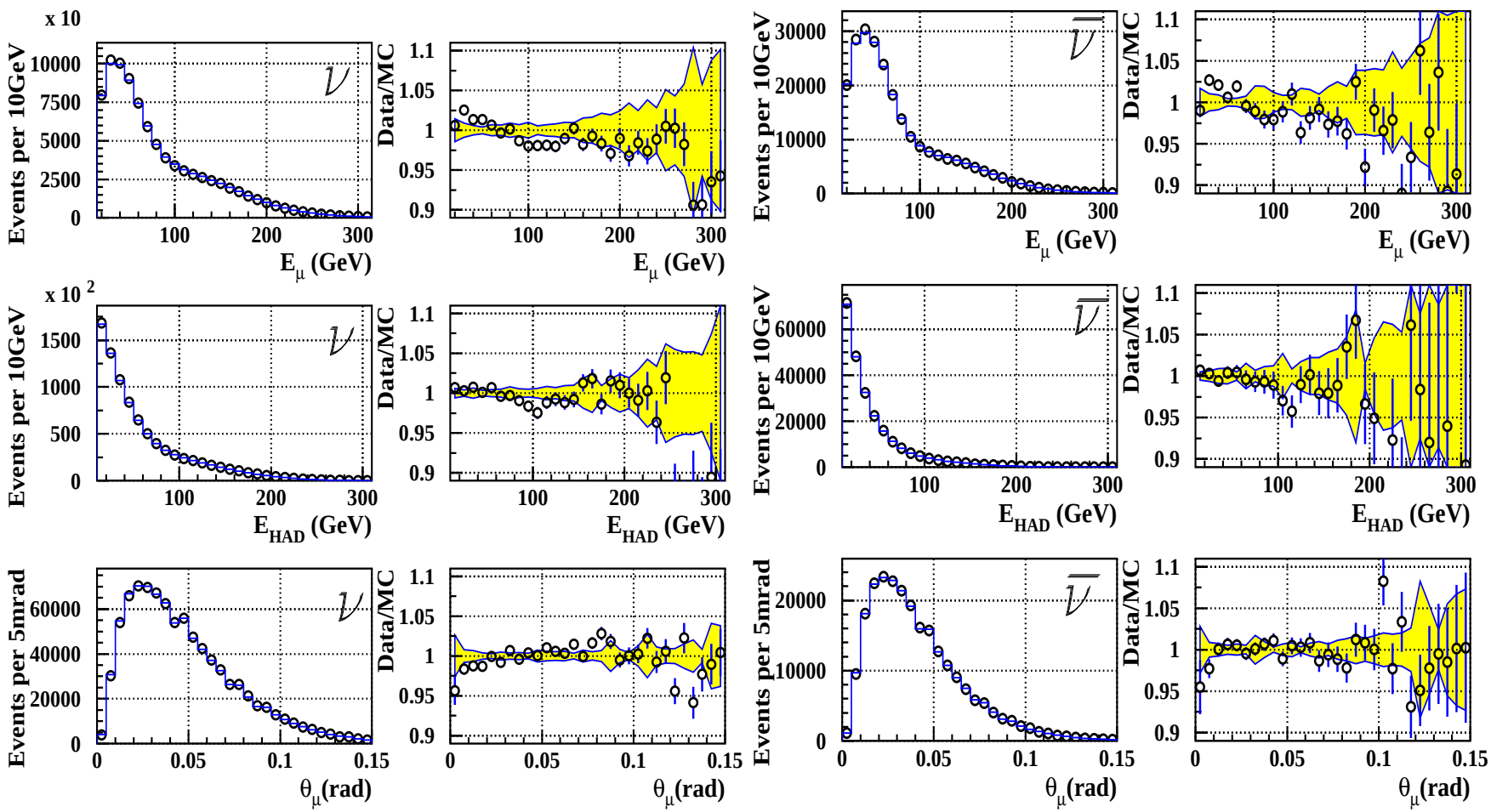

- Monte Carlo Describes the data well over entire kinematic range. (χ^2/dof=2225/2599)
  - E_μ and $E_{\rm HAD}$ Smearing parameterized from Test beam measurements.
  - θ_μ from Geant Detector simulation.

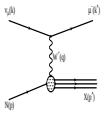

Cross Section Systematic Uncertainties

7 systematic uncertainty sources considered:

- E_μ and $E_{\rm HAD}$ scales *(affect both cross section and flux extraction)*
- m_c and $\frac{B}{A}$ *(are important for the flux extraction*. m_c=1.4$\pm$0.18.
- E_μ and $E_{\rm HAD}$ smearing models. *(important at high energy).*
- Cross section model uncertainty *(small).*
- overall normalization uncertainty 2.1% *(from uncertainty in world average absolute cross section at high energy.)*

Provide a point-to-point covariance matrix:

$$M_{\alpha\beta} = \sum_i^7 \delta_{i|\alpha}\delta_{i|\beta}$$

- $\delta_{i|\alpha}$ is the 1σ shift in data point α due to systematic uncertainty i of size ϵ_i.

$$\delta_{i|\alpha} = \frac{\frac{d^2\sigma}{dxdy}(+\epsilon_i) - \frac{d^2\sigma}{dxdy}(-\epsilon_i)}{2}$$

► χ^2 including all systematic uncertainties:

$$\chi^2 = \sum_{\alpha\beta}(D_\alpha - f_\alpha^{theory})M^{-1}_{\alpha\beta}(D_\beta - f_\beta^{theory})$$

- $M_{\alpha\beta}$ is point to point covariance matrix:
- D_α - measured differential cross section
- f_α^{theory} - the model prediction

NuTeV Differential Cross Section

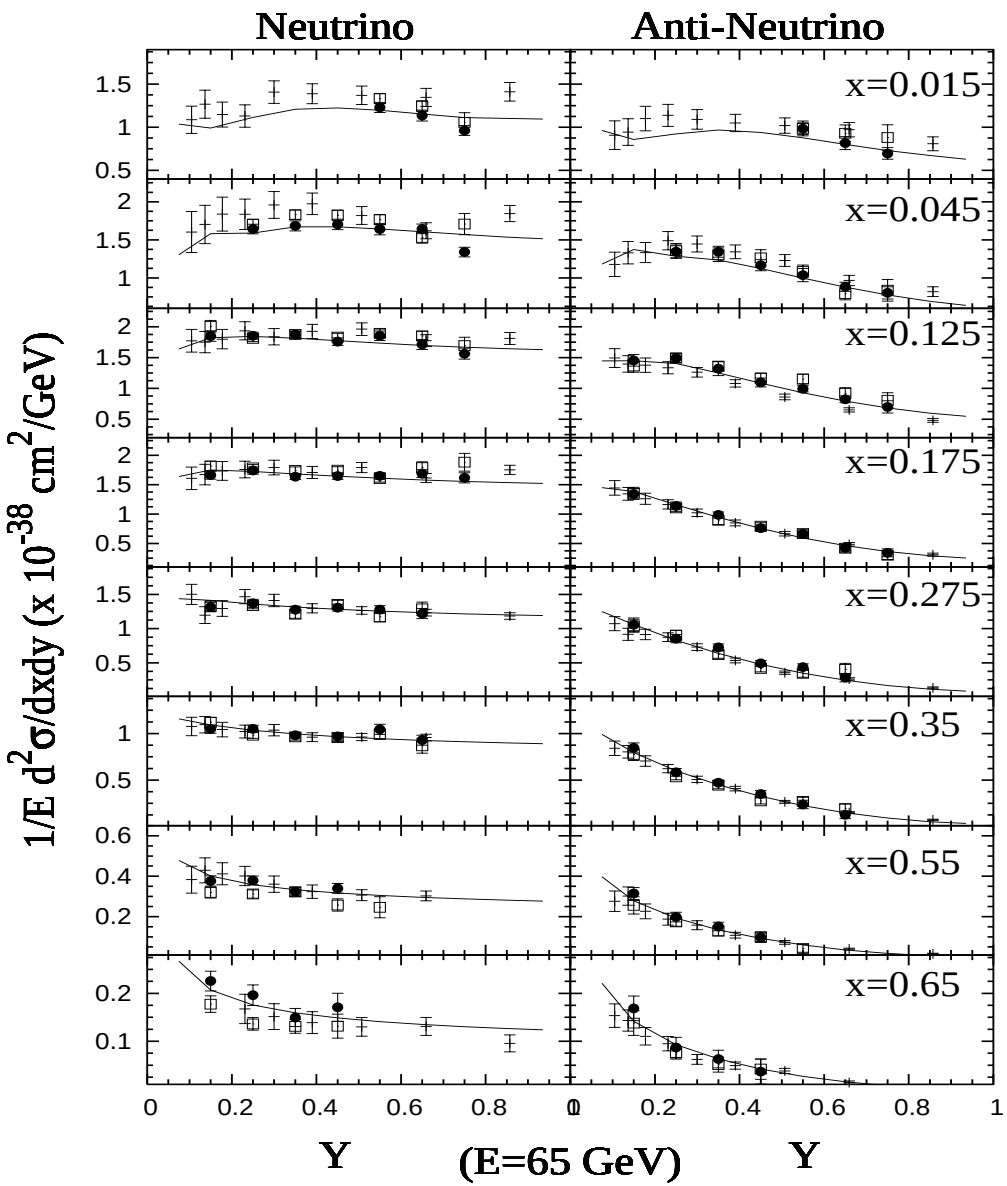

- Extracted $\nu(\overline{\nu}) - Fe$ Cross-Sections in x bins
  $E_\nu = 65$ GeV

NuTeV	●
CCFR	□
CDHSW	+

  - CDHSW [Z. Phys C49 187, 1991]
  - CCFR [PRL 86 2742, 2001, U.K Yang, Thesis]

- Better control of largest systematic uncertainties:

	E_μ scale	E_{had}	E_ν range
CDHSW	2%	2.5%	20-200 GeV
CCFR	1%	1%	30-400 GeV
NuTeV	0.7%	0.43%	30-350 GeV

NuTeV Differential Cross Section

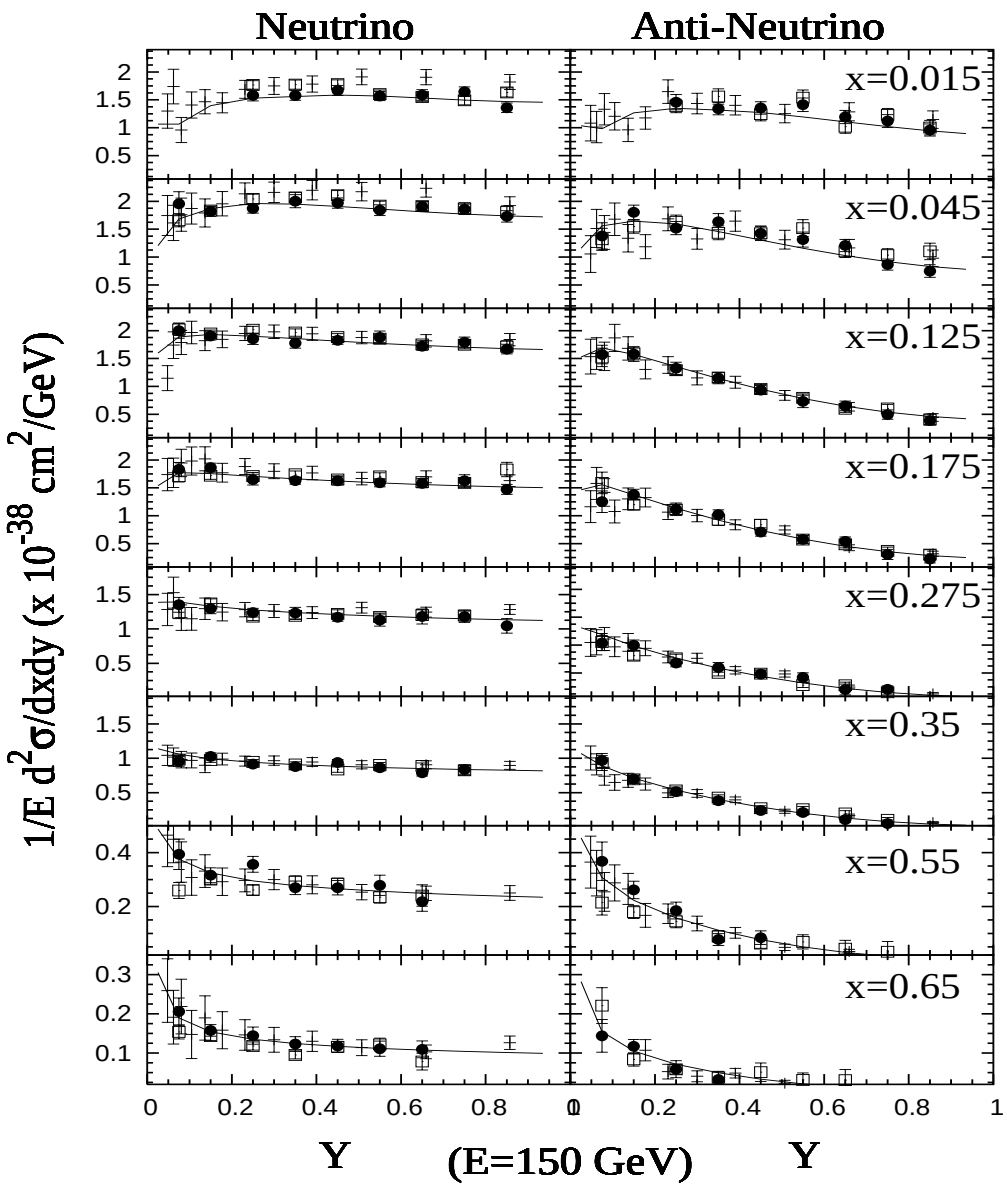

- Extracted $\nu(\overline{\nu}) - Fe$ Cross-Sections in x bins
  $E_\nu = 65$ GeV & 150 GeV

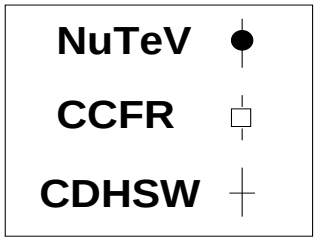

  - CDHSW [Z. Phys C49 187, 1991]
  - CCFR [PRL 86 2742, 2001, U.K Yang, Thesis]

- Better control of largest systematic uncertainties:

	E_μ scale	E_{had}	E_ν range
CDHSW	2%	2.5%	20-200 GeV
CCFR	1%	1%	30-400 GeV
NuTeV	0.7%	0.43%	30-350 GeV

Neutrino Data Comparison

Low and moderate x ($0.015 < x < 0.40$)

- CCFR: Shape and level agree well.
- CDHSW: Level agrees, shape differs from both CCFR&NuTeV. *(known problem with CDHSW).*

High x ($x > 0.45$)

- CCFR consistently lower, *discrepancy increases with x*: **4% (x=0.45) → 18% (x=0.65)**
- CDHSW level in agreement w/both CCFR&NuTeV.

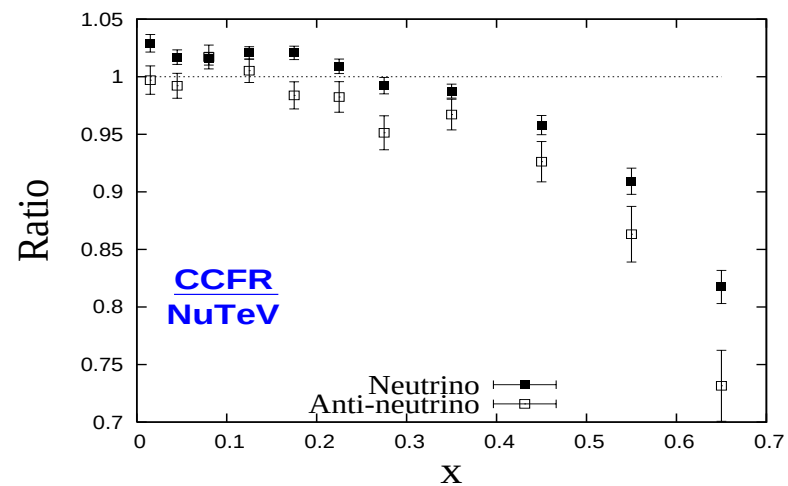

NuTeV vs. CCFR

- **Similar detectors and techniques.**

(1) NuTeV separate ν and $\overline{\nu}$/ CCFR simultaneous ν and $\overline{\nu}$.

- NuTeV always focusing "right-sign" μ (*better acceptance*)
- CCFR focusing $50\%\ \mu^+ / 50\%\ \mu^-$

(2) NuTeV continuous calibration/ CCFR 2 calibration runs.

- NuTeV mapped hadron and muon response,⇒ better calibrated toroid and calorimeter.

Investigating the source of discrepancy:

- Largest single contribution is due to the difference in NuTeV/CCFR magnetic fi eld maps. Difference corresponds to a 0.8% shift in muon energy scale: ⇒ effect ∼6% for x=0.65
- Other effects (decrease NuTeV at high-x)

Different model fi t parameters	3%
Different muon smearing model	2%
Hadron energy non-linearity	1-2%

Accounts for ∼12% out of 18% difference at x=0.65.

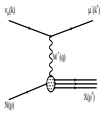

Extraction of Structure Function $F_2(x, Q^2)$

$$\left[\frac{d^2\sigma^\nu}{dxdy}+\frac{d^2\sigma^{\overline{\nu}}}{dxdy}\right]\frac{\pi}{2MG^2E_\nu} = \left(1-y-\frac{Mxy}{2E}+\frac{1+\left(\frac{2Mx}{Q}\right)^2}{1+R_L}\frac{y^2}{2}\right)F_2+y(1-\frac{y}{2})\Delta xF_3$$

- Model inputs
  - $R_L(x, Q^2)$ [L.W.Whitlow $et.al.$ Phys.Lett. B250(1990)]
  - $\Delta xF_3(x, Q^2)$ [R.Thorne and R.Roberts, Phys.Lett. B 421 (1998)]
- Fit determines $F_2(x, Q^2)$

  $F_2(x, Q^2) = \frac{1}{2}\left(F_2^\nu(x, Q^2) + F_2^{\overline{\nu}}(x, Q^2)\right)$
- Cross-Sections corrected to :
  - Isoscalar target

    (5.67% excess of n over p in Fe target)
- QED radiative corrections applied

  [D.Y.Bardin and Douchaeva,JINR-E2-86-260(1986)]

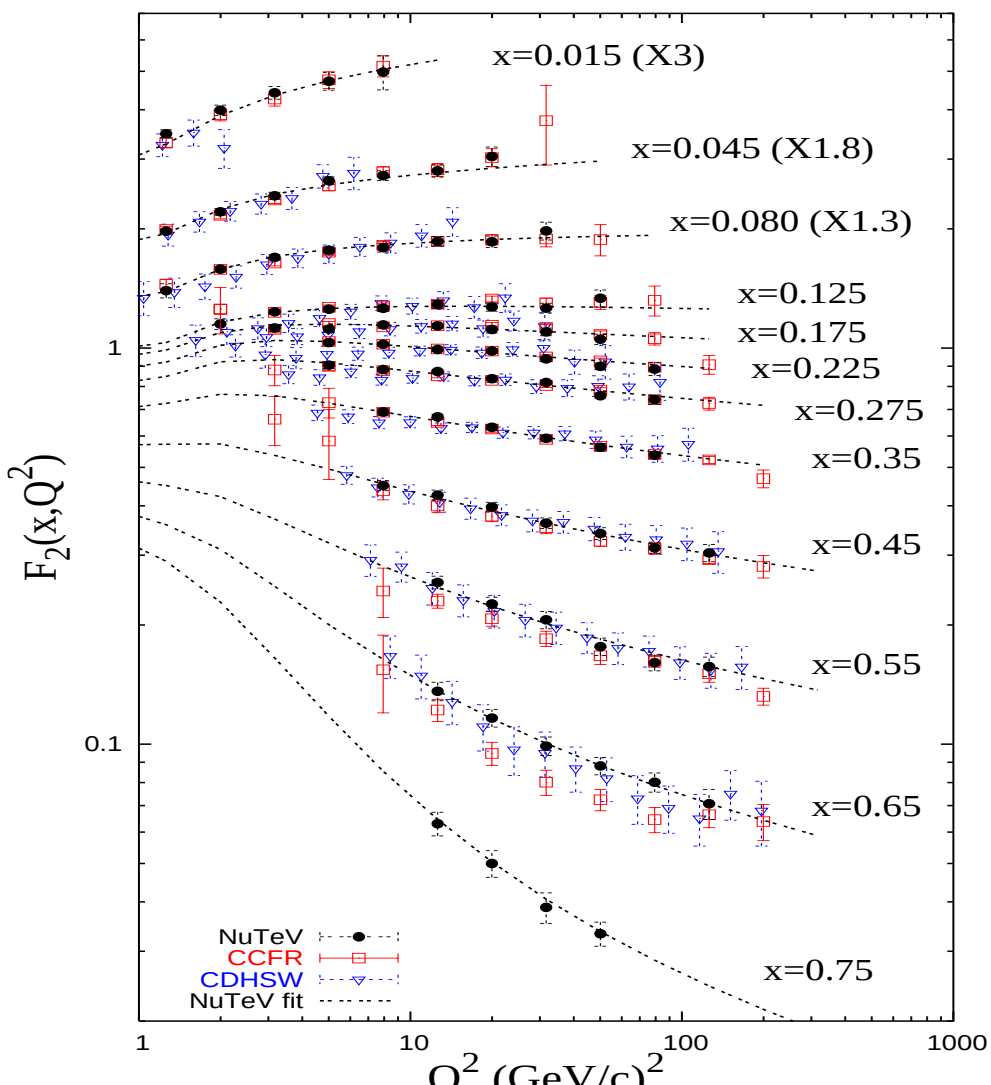

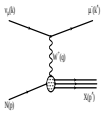

Extraction of Structure Function $xF_3(x, Q^2)$

$$\left[\frac{d^2\sigma^\nu}{dxdy} - \frac{d^2\sigma^{\overline{\nu}}}{dxdy}\right]\frac{\pi}{2MG^2E_\nu} = \Delta F_2\left(1 - y - \frac{Mxy}{2E} + \frac{1+\left(\frac{2Mx}{Q}\right)^2}{1+R_L}\frac{y^2}{2}\right) + \left(y - \frac{y^2}{2}\right)xF_3 \approx \left(y - \frac{y^2}{2}\right)xF_3$$

- Fit determines $xF_3(x, Q^2)$
  $xF_3(x, Q^2) = \frac{1}{2}\left(xF_3^\nu(x, Q^2) + xF_3^{\overline{\nu}}(x, Q^2)\right)$
  $\Delta F_2 \sim 0 \Rightarrow$ no inputs required.

- Cross-Sections corrected to :
  - Isoscalar target
    (5.67% excess of n over p in Fe target)
- QED radiative corrections applied

[D.Y.Bardin and Dokuchaeva,JINR-E2-86-260(1986)]

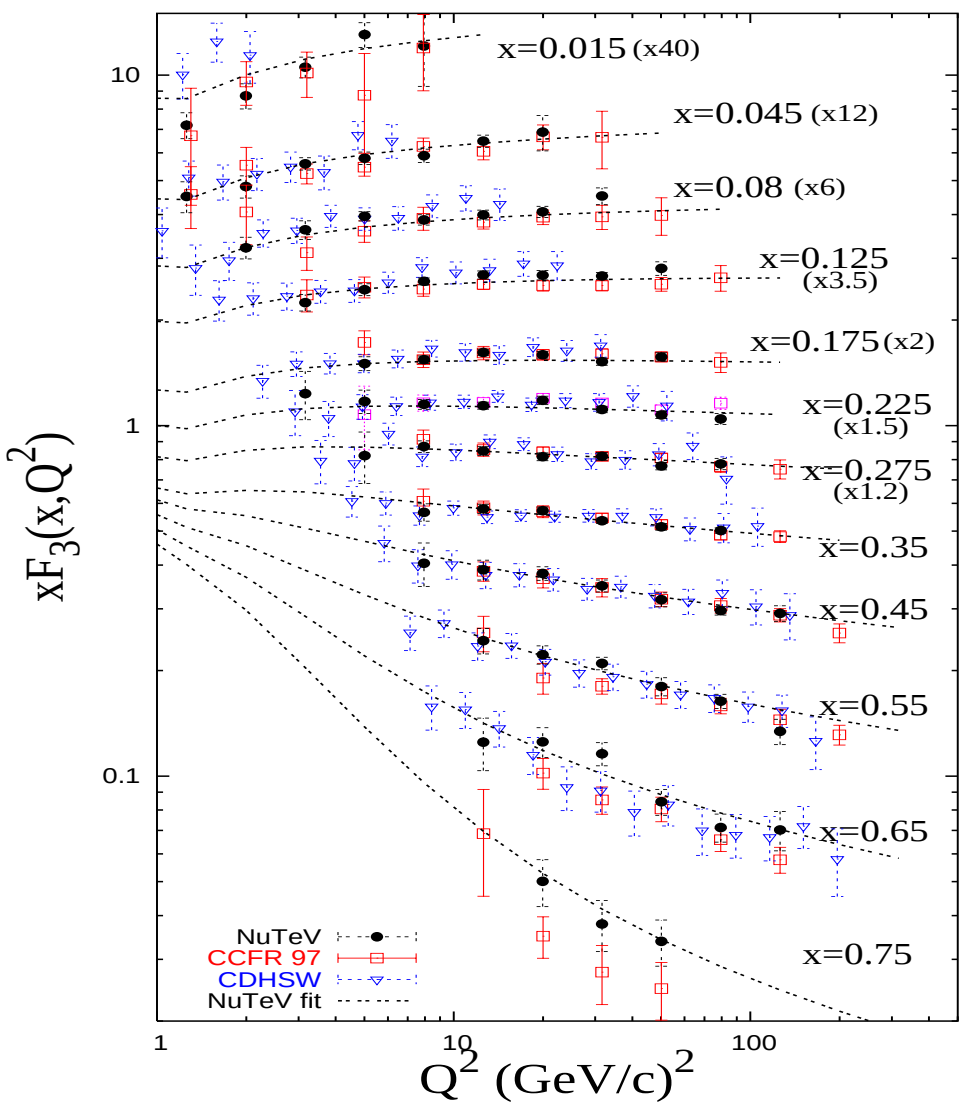

Comparison to NLO Theory Models

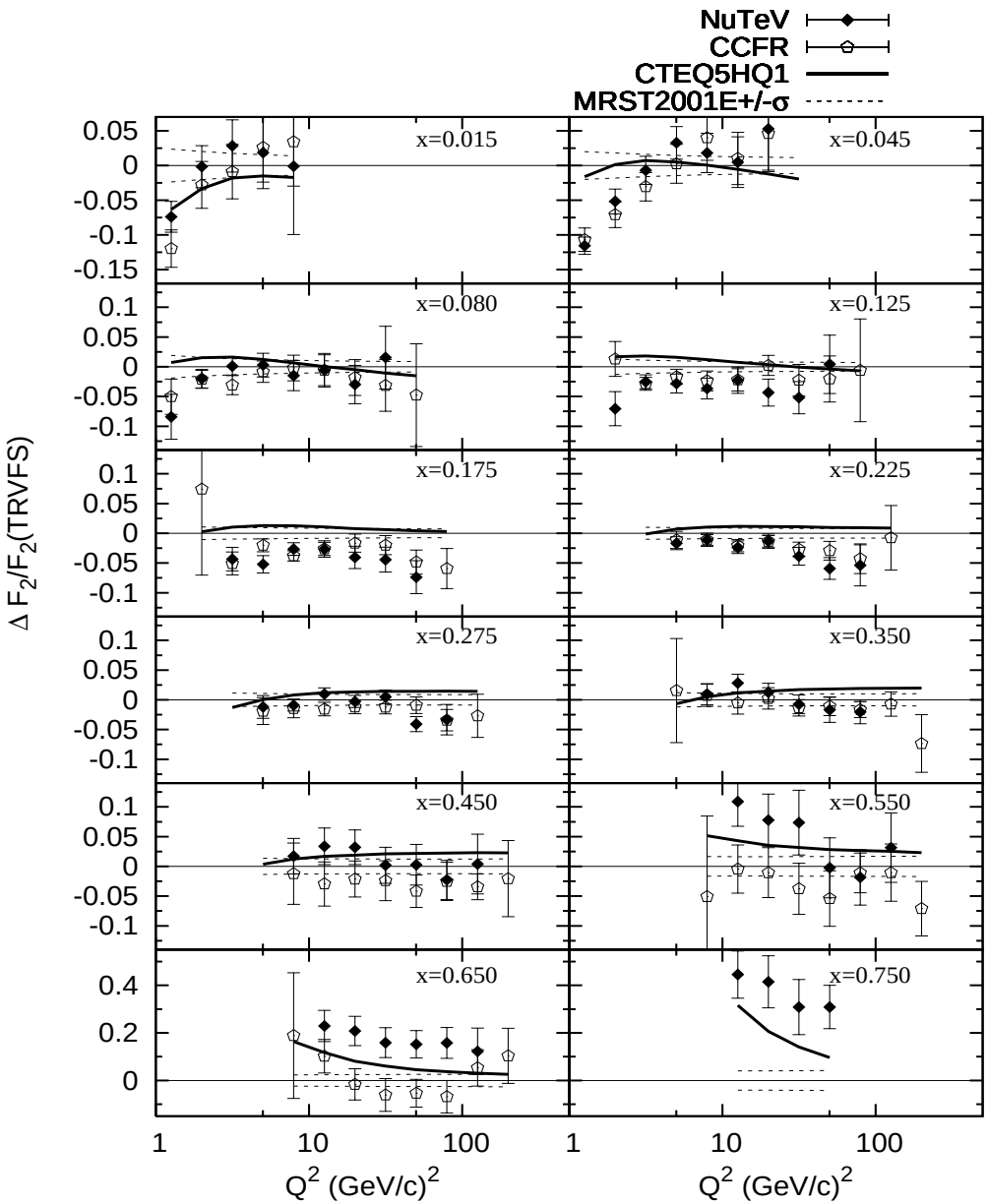

$$\frac{F_2^{\mathrm{DATA}} - F_2^{Theory}}{F_2^{Theory}}$$

- Theory models:
  - ACOT(CTEQ5HQ1)
  - TRVFS(MRST2001E)
- Theory curves are corrected for
  - Target-mass effects [H. Georgi and H. Politzer, Phys. Rev. D14, 1829].
  - Nuclear effects: using a fi t to charged-lepton measurements.
- Good agreement at moderate x.
- Q^2 dependent disagreement at low-x.
- NuTeV is above theory at high-x.
  - CCFR agrees better (slightly below) but was used in global fi ts.

NLO QCD Fits *(NEW)*

- Λ_{QCD} determined from NLO QCD fits
  - Non-singlet $xF_3(x, Q^2)$ only $\star$ evolution independent of gluon distribution.
  - Combined $F_2(x, Q^2)$ and $xF_3(x, Q^2)$ $\star$ greater statistical precision.
- NLO model with improved treatment of heavy quark production

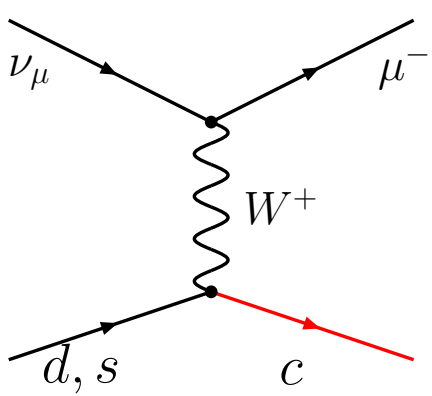

$m_c = 1.4$ GeV $\sim Q$

- Previous experiments used a LO model to correct data
- Aivazis-Collins-Olness-Tung (ACOT) scheme: accounts for quark masses [F. Olness, S. Kretzer]
  - belongs to VFN factorization schemes

- Evolution starts at $Q_0^2 = 5$ GeV^2, [Data $Q^2 > 5$GeV^2, $W^2 > 10$GeV^2]
  - Λ_{QCD} enters as a free parameter via DGLAP evolution equations
  - Using code from F. Olness (heavy quark prod.) and J. Owens (QCD fi t)

NuTeV α_s Result

- Non-singlet Fit Result:
  $\alpha_S(M_Z) = 0.1260 \pm 0.0028(exp)^{+0.0034}_{-0.0050}(th)$
- $F_2 + xF_3$ Fit Result:
  $\alpha_S(M_Z) = 0.1247 \pm 0.0020(exp)^{+0.0030}_{-0.0047}(th)$
- NuTeV result:
  - Above world average, within 1σ agreement.
    WEIGHTED WORLD AVERAGE:
    $\alpha_S(M_Z) = 0.1185 \pm 0.0020$ [PDG 2005]
  - One of the most precise measurements.

  Largest uncertainties :
  - Expt: E_μ and $E_{\rm HAD}$ energy scales.
  - Theor.: Scale dependence: μ_R and μ_F
    $\mu_F^2 = C_i Q^2$, $C_i = 1/2, 1, 2$

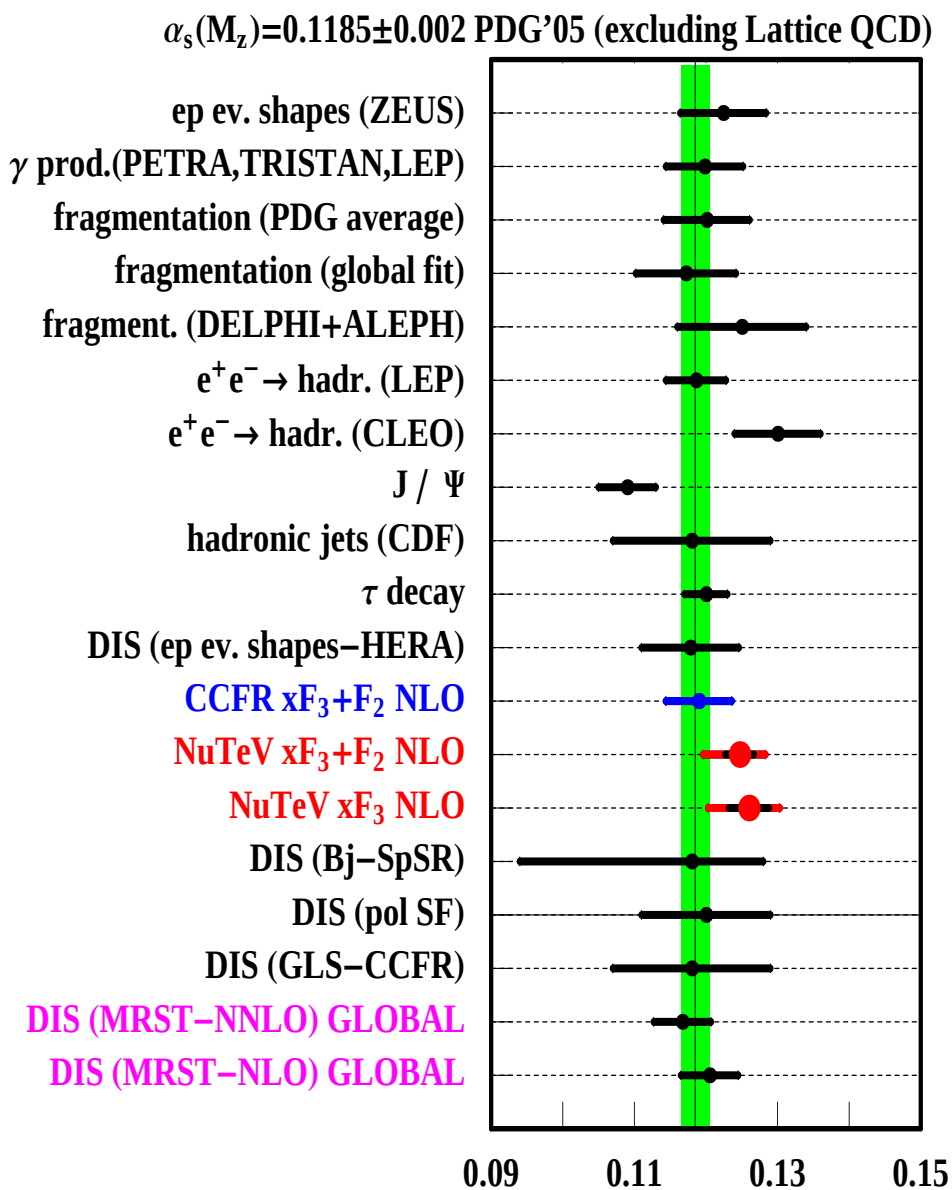

Ref: V. Radescu, PhD Thesis, University of Pittsburgh, 2006.

NuTeV Summary

- NuTeV has extracted the precise $\nu - Fe$ differential cross sections in the energy range $E_\nu > 30$ GeV:
  - [Phys. Rev. D 74, 012008 (2006)]
  - Improved understanding of the systematic uncertainties:
    - ⋆ $\frac{\delta E_\mu}{E_\mu} = 0.7\%$
    - ⋆ $\frac{\delta E_{had}}{E_{had}} = 0.43\%$
- Structure Functions $F_2(x, Q^2)$ and $xF_3(x, Q^2)$ have been presented.
  - Used to make a precise measurement of α_s at low Q^2.

Neutrino Comparison Summary

- Good agreement with previous νN for moderate x ($x < 0.4$).
- Systematically above previous precise result (CCFR) at high-x: **4% (x=0.45)** $\rightarrow$ **18% (x=0.65)**
  - Large fraction of this difference understood $\longrightarrow$ due to muon momentum calibration improvements in NuTeV.

Chorus Experiment

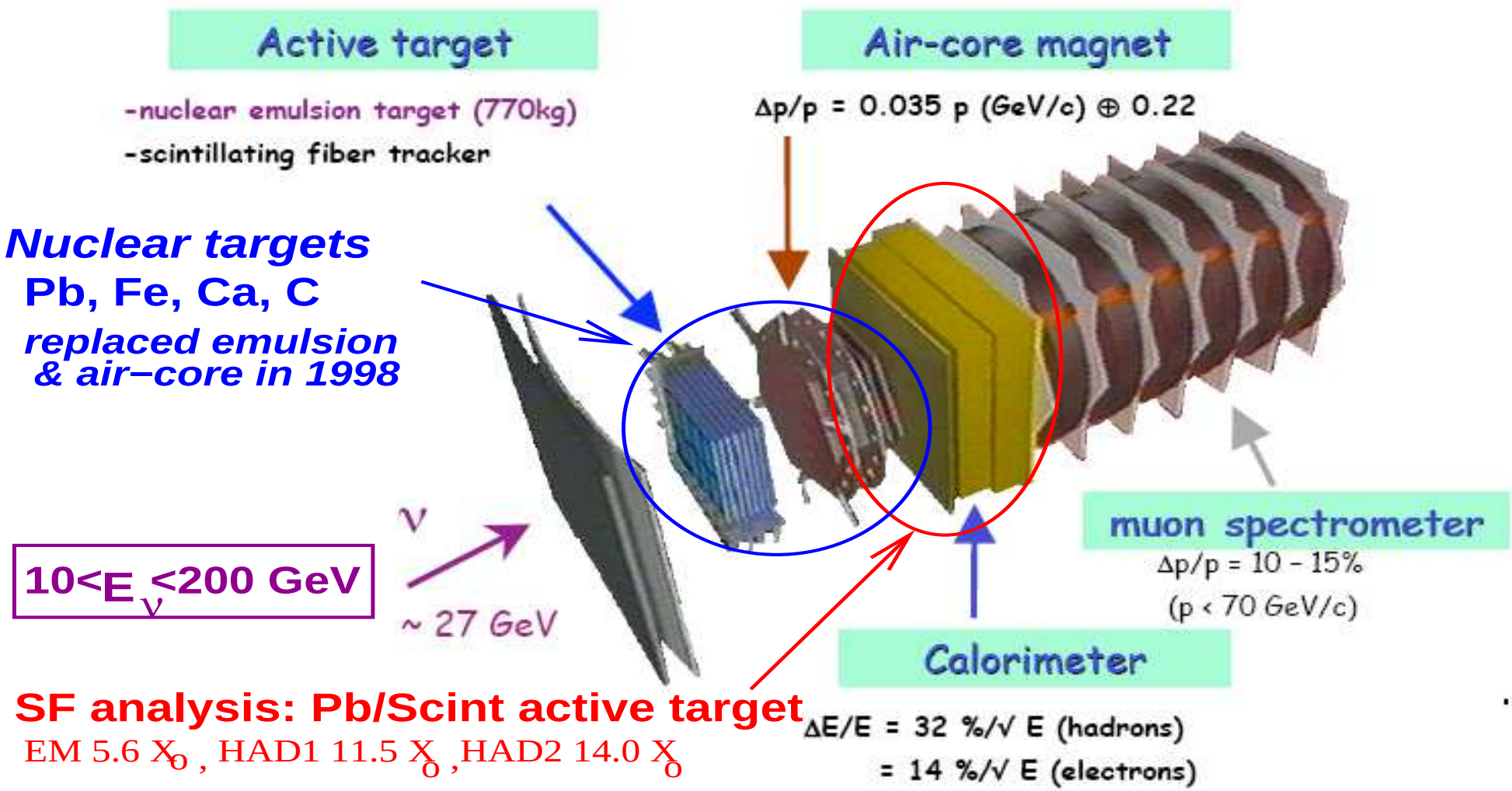

SF analysis: Pb/Scint active target

EM 5.6 X_0 , HAD1 11.5 X_0 ,HAD2 14.0 X_0

- Results on ν-Pb and $\overline{\nu}$-Pb differential cross section and structure functions: Phys. Lett B 632 (2006) 65.
- http://choruswww.cern.ch/Publications/papers.html for other cross section results.

Chorus ν-Pb Structure Functions

- DIS events samples:
  $E_\mu > 5$ GeV, $4 < E_{\rm HAD} < 100$ GeV
  - 870K ν
  - 146K $\overline{\nu}$ (Dedicated $\overline{\nu}$ running with μ^+ focusing).
- Systematic uncertainties:
  - E_μ scale 2.5%
  - $E_{\rm HAD}$ scale 5.0% (test beam exposure)

First measurement of Pb structure functions

- Comparison with ν-Fe:

  CCFR97: Seligman et. al. , PRL 79 1213, 1997

  CDHSW: Berge et al. Z. Phys C49 187, 1991

  - Caveat: Nuclear effects could differ

- $F_2(x, Q^2)$: favors CCFR97 over CDHSW.
  CDHSW Q^2 shape differs $0.08 < x < 0.35$.
  - *Nuclear effect differences Pb vs. Fe are small.*

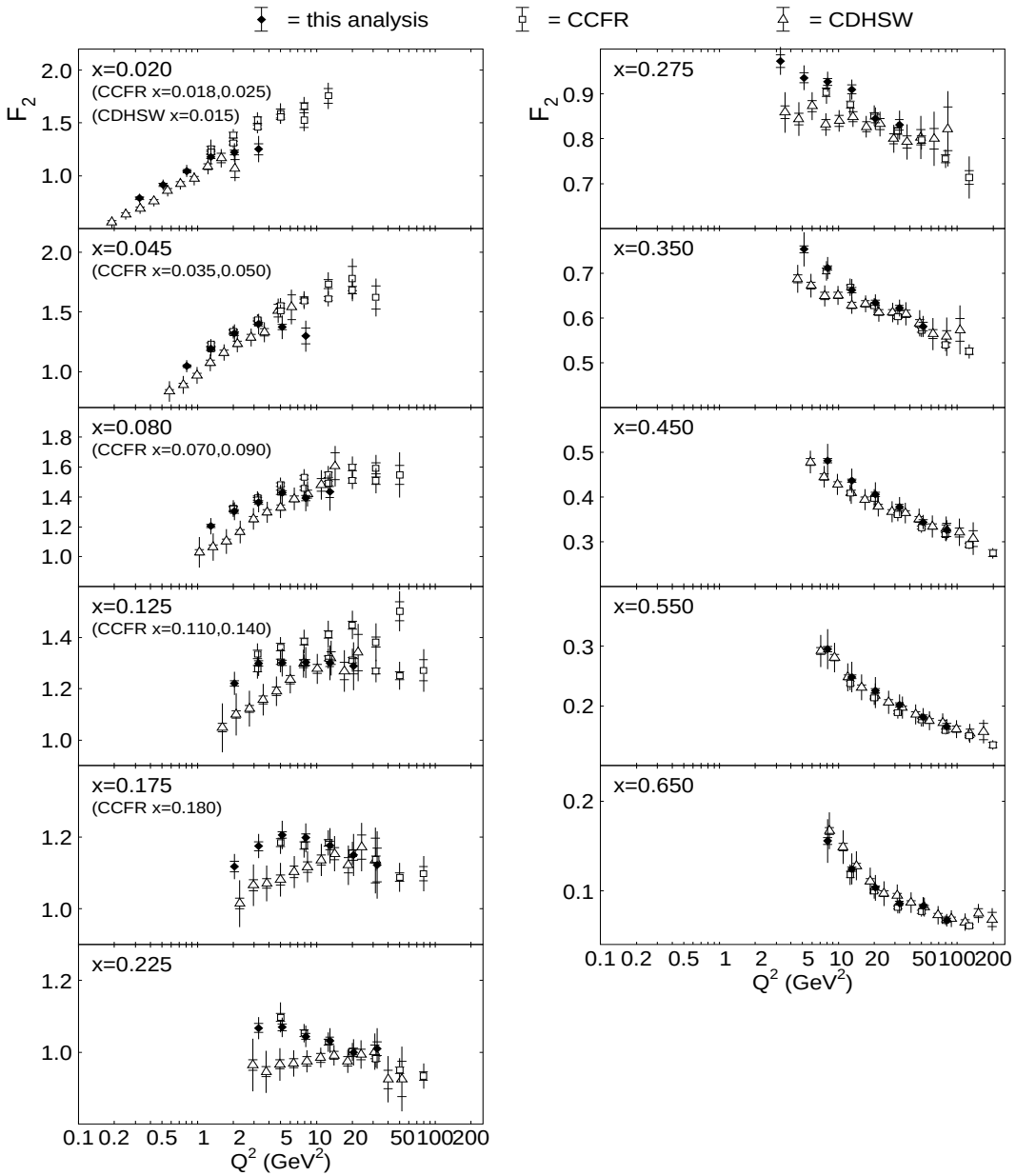

Chorus ν-Pb Structure Functions

- DIS events samples:
  $E_\mu > 5$ GeV, $4 < E_{\rm HAD} < 100$ GeV
  - 870K ν
  - 146K $\overline{\nu}$ (Dedicated $\overline{\nu}$ running with μ^+ focusing).
- Systematic uncertainties:
  - E_μ scale 2.5%
  - $E_{\rm HAD}$ scale 5.0% (test beam exposure)

First measurement of Pb structure functions

- Comparison with ν-Fe:

  CCFR97: Seligman et. al. , PRL 79 1213, 1997

  CDHSW: Berge et al. Z. Phys C49 187, 1991

  - Caveat: Nuclear effects could differ

- $xF_3(x, Q^2)$: agrees with both experiments.
  - *Nuclear effect differences Pb vs. Fe are small.*

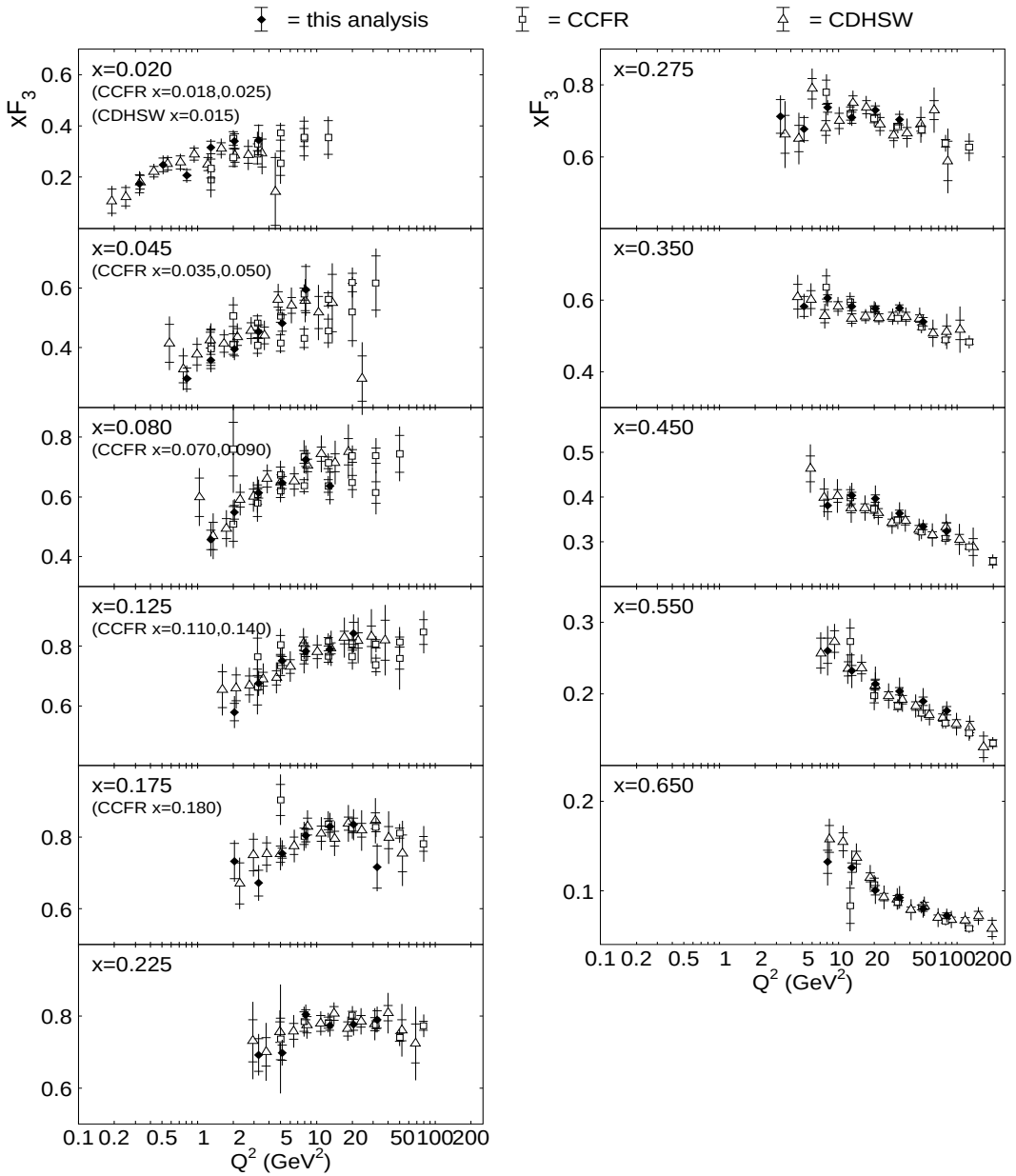

Comparison with NuTeV

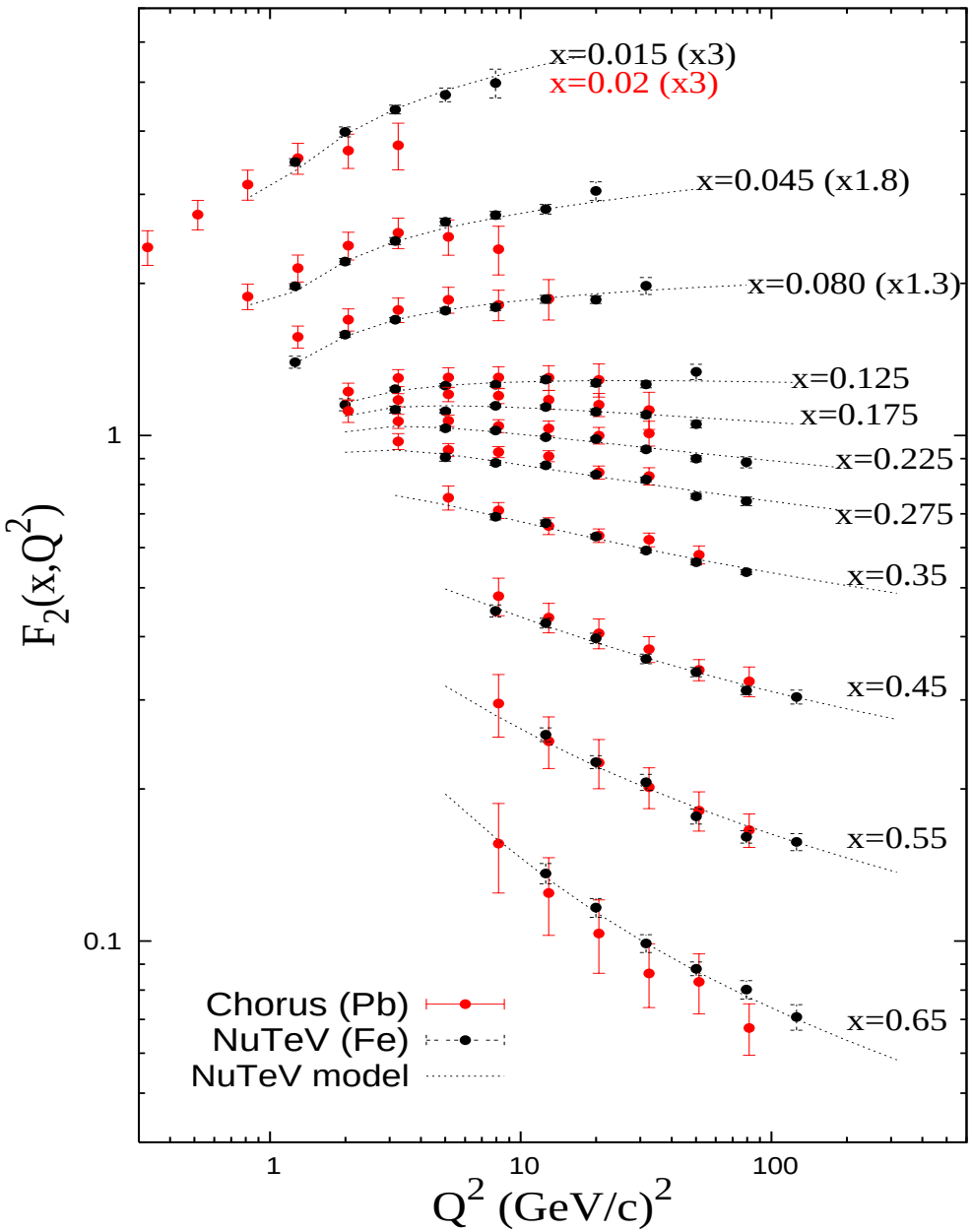

- Good agreement with NuTeV over all x.
  - Hint of shape difference at low x and low Q^2 ($x < 0.175$)
  - more High-x ⟶

High-x Comparison

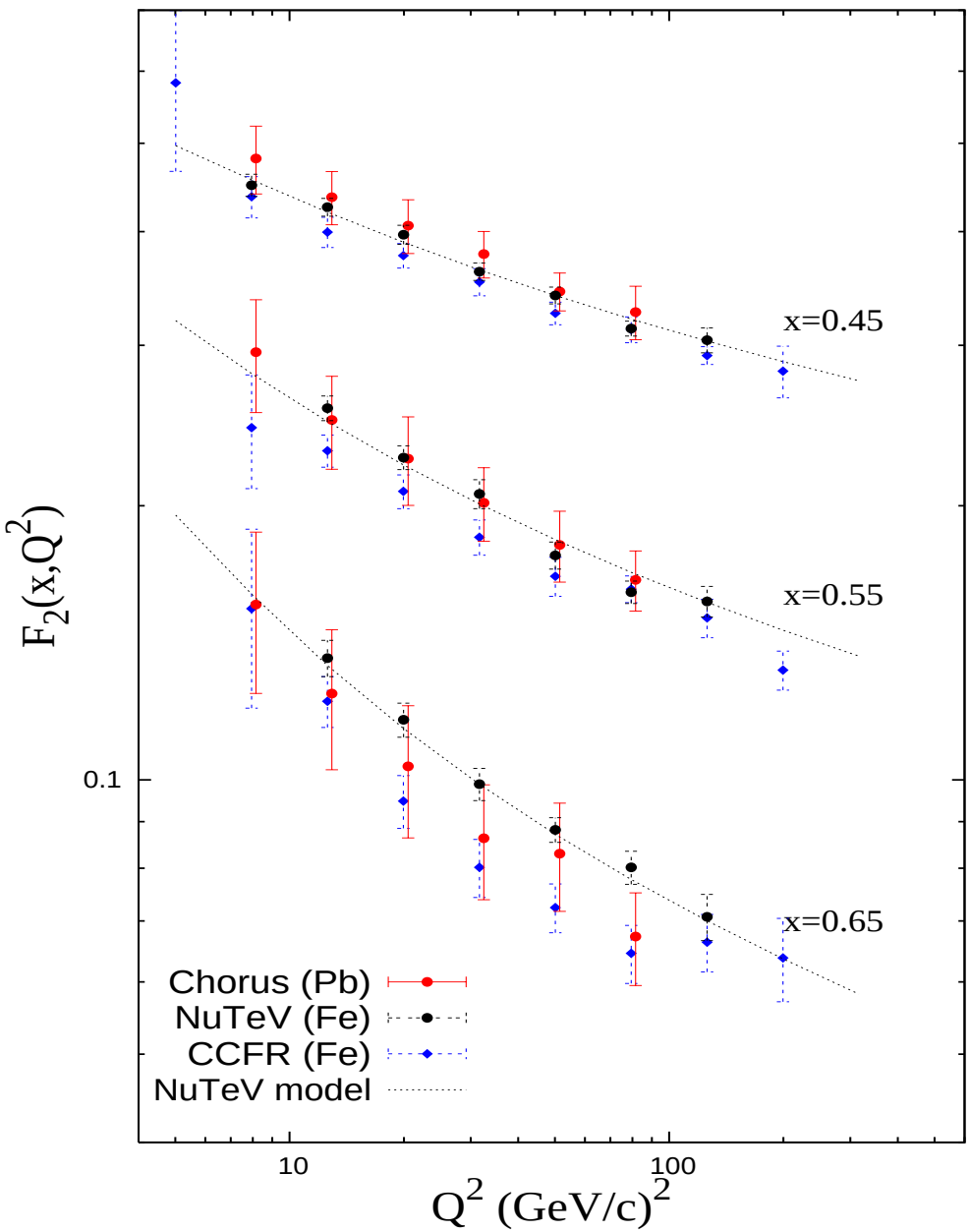

- (Blue points) Comparison with CCFR01: [PRL 86 2742, 2001, U.K Yang, Thesis] (Chorus plot shows CCFR97)
- In good agreement with both NuTeV and CCFR. *(better agreement with NuTeV for x=0.45, 0.55 bins)*
  - *CHORUS not as precise.*

DIS Cross Sections at NOMAD

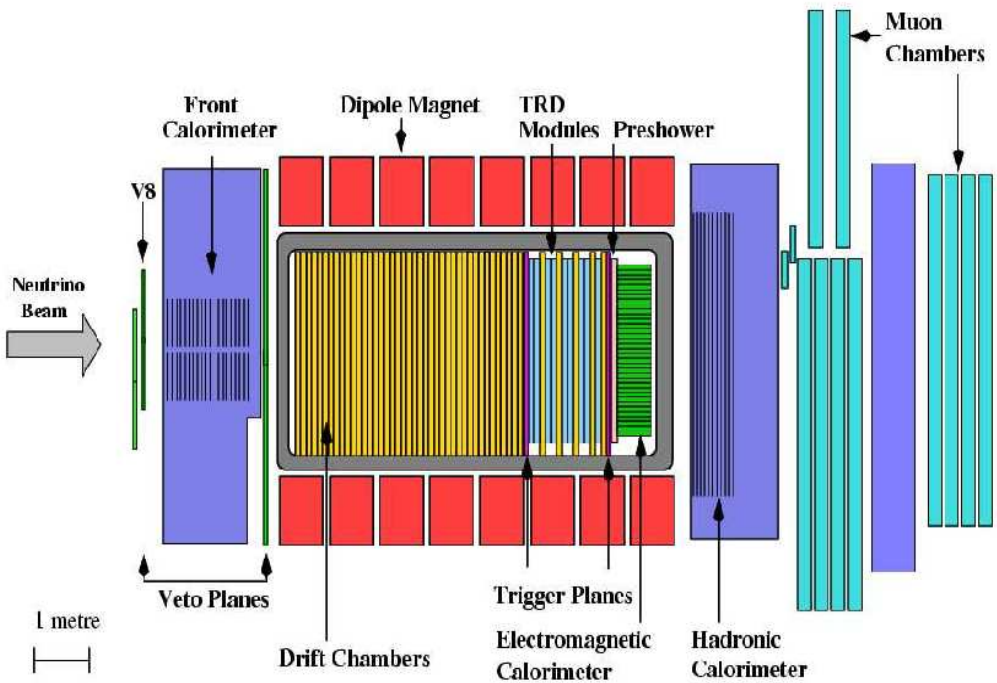

The NOMAD detector

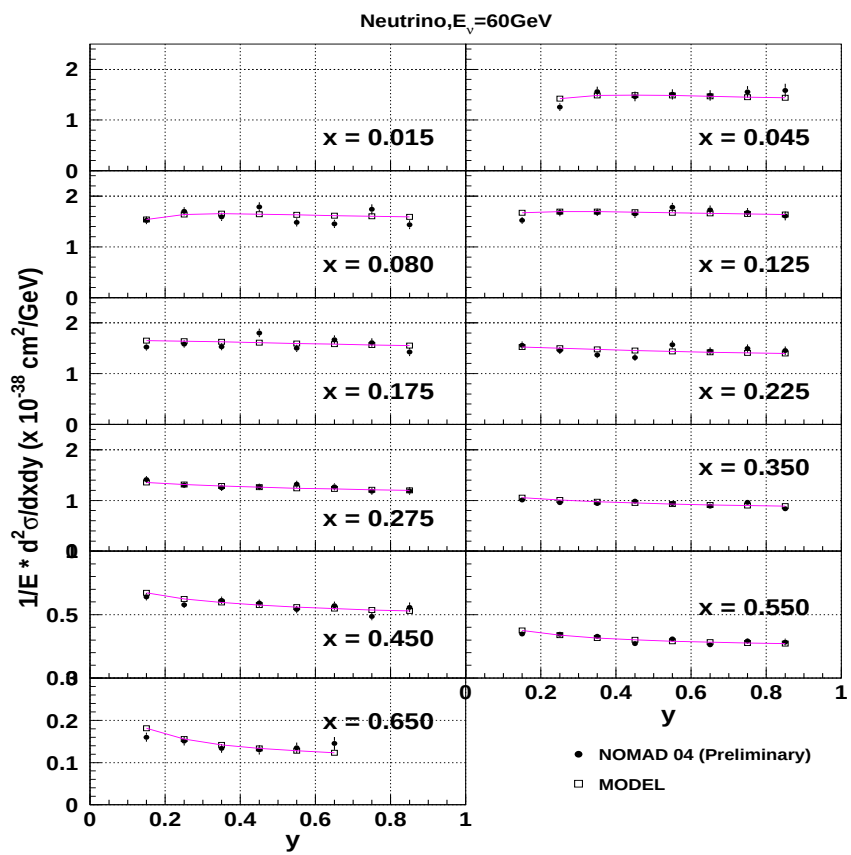

- Fine-grained spectrometer: matching bubble chamber reconstruction quality.
- 10<E_ν<200 GeV, $\langle Q^2 \rangle \sim$ 13 GeV^2
  - Carbon (1.3M), Fe (12M), and Al (1.5M)
  - Dimuon sample near charm threshold.
- Preliminary differential cross section results (R. Petti)
  - First high-statistics data on Carbon target.

Future Low Energy

MINOS, Minerνa

DIS at NuMI

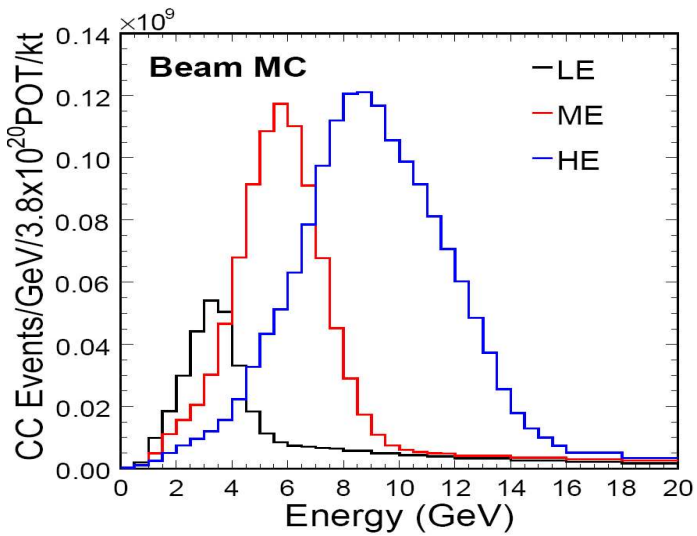

- Movable target, allows three beam configurations, LE, ME, and HE.
- ⋆ Energy range covers interesting region: QE, Resonance and DIS all contribute.

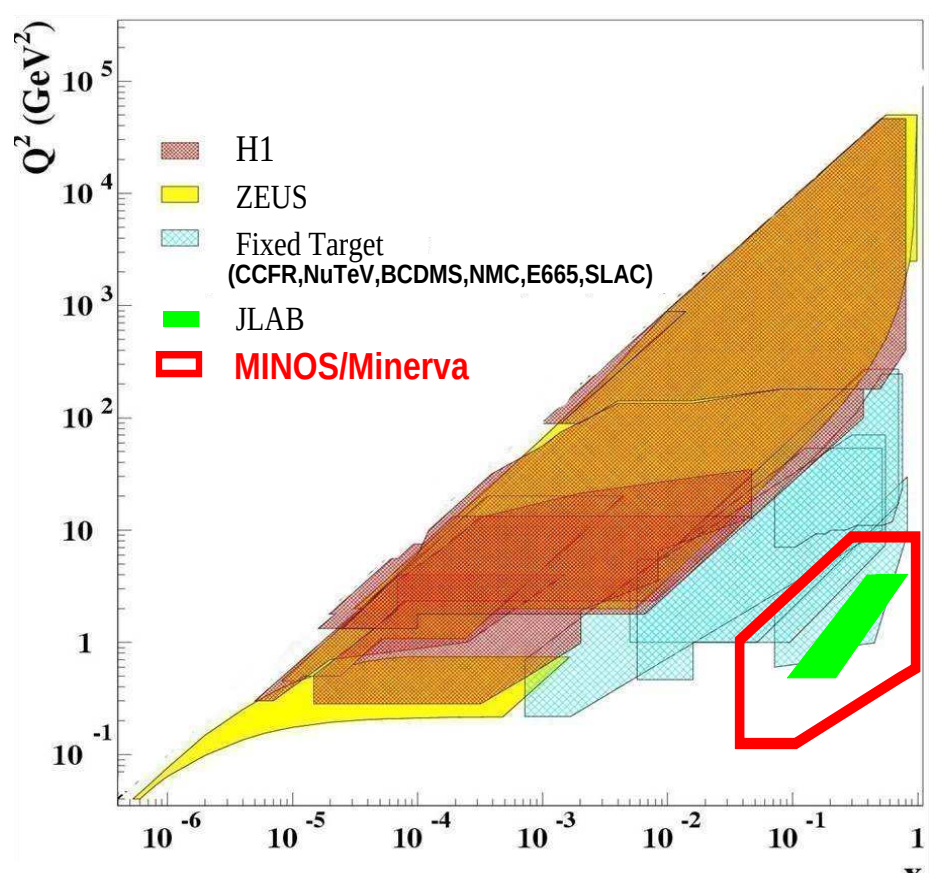

- ⋆ New kinematic regime for ν N SFs
- ⋆ High-x low Q^2 : Good coverage in charged-lepton scattering, but little neutrino data.

MINOS Near Detector Data

- MINOS Near detector → *largest data sample for neutrino interactions in this energy range to date.*
- **Majority of data ($\sim$ 95%) taken in low energy configuration (LE-10).**
  - LE-10 Event Composition: 92.9%ν_μ 5.8% $\overline{\nu_\mu}$, 1.3% $(\nu_e + \overline{\nu_e})$

Near CC events (May 2007).

Beam	Target z (cm)	CC Sample
LE-10	**-10**	**3.7** $\times$ **10**$^{\mathbf{6}}$ (ν)
LE-10	**-10**	**3.0** $\times$**10**$^{\mathbf{5}}$ $(\overline{\nu})$
ME	-100	1.9 $\times 10^4$
HE	-250	3.7 $\times 10^4$

Exposure of 3.0E20 PoT

- DIS is the largest contribution:

  DIS 62%, RES 21%, QE 17%

  → dominates for $E_\nu > 5$ GeV.
- **Flux, cross section, and SF analyses underway.**

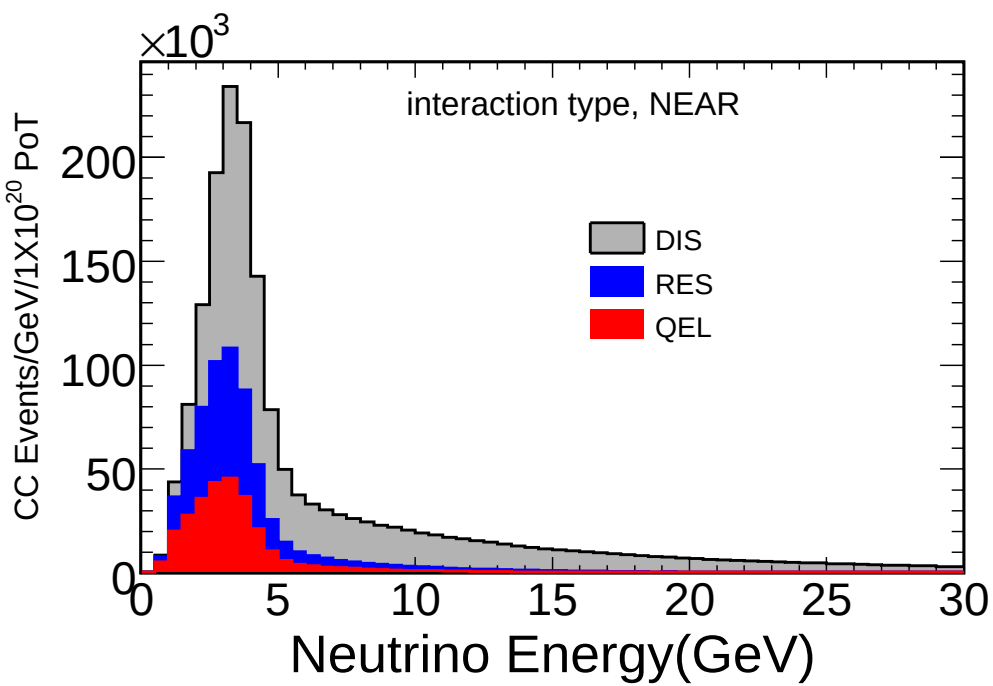

CC Flux and Cross Section Analysis

CC Event Selection

- Good track with $E_\mu > 2$GeV.
  - Stopping, momentum from range
  - Exiting, momentum from fi t
- Contained vertex in upstream 'target' region (Fid. mass $\sim$4ton.)
- Separate ν_μ and $\overline{\nu_\mu}$ using μ sign.

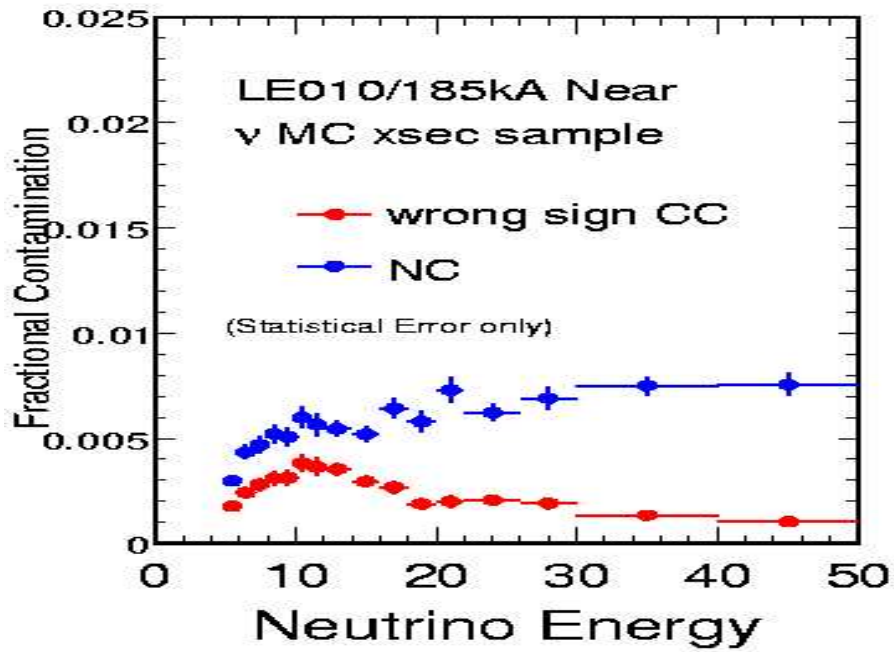

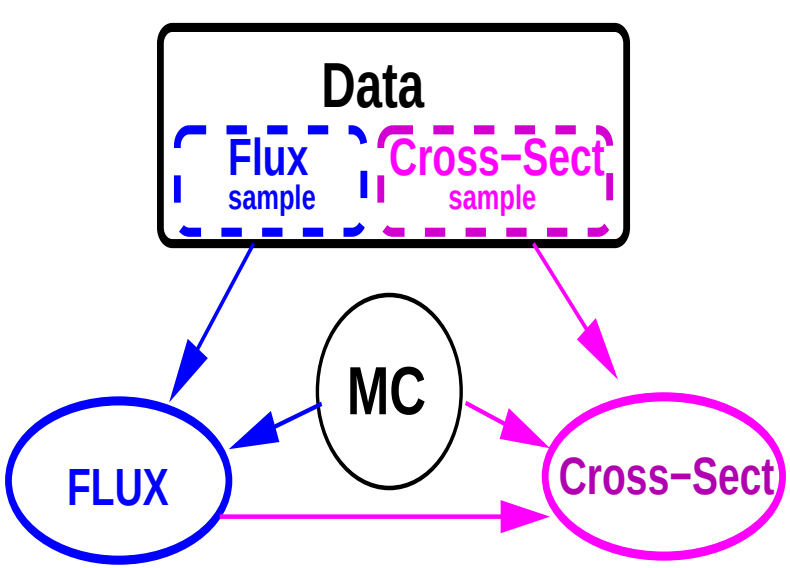

- Flux, and Cross Section *extracted using an iterative technique.*

Monte Carlo Ingredients

- Input beam flux (GEANT3 based beamline simulation, production model FLUKA05).
- Cross section model (NEUGEN3): uses Bodek-Yang duality model,(BY-GRV98LO), tuned to data in DIS/res. overlap region.
- Detector simulation (tuned GEANT3).

Flux and Cross Section Extraction

- Use inclusive low $\nu(= E_{\mathrm{HAD}})$ cross section to get flux shape. $\rightarrow \Phi(\mathrm{E}) \propto \mathrm{N}(\mathrm{E}, \nu < \nu_{\mathrm{o}})$.
  - *Same method used at higher energy (CCFR/NuTeV)$\rightarrow$ adapted to lower energies.*

Flux

1. $\nu < \nu_o = 1$GeV for 5$< E_\nu <$10GeV,
   $\nu < \nu_o = 2$GeV for $E_\nu > 10$GeV
2. Use cross section model to correct for energy dependence in low-ν sample, $c(\mathrm{E}) = \frac{\sigma_{\mathrm{E}\rightarrow\infty}(\nu<\nu_o)}{\sigma(\nu<\nu_o)}$
3. $\Phi(\mathrm{E}) \propto c(\mathrm{E})\mathrm{N}(\mathrm{E}, \nu < \nu_{\mathrm{o}})$

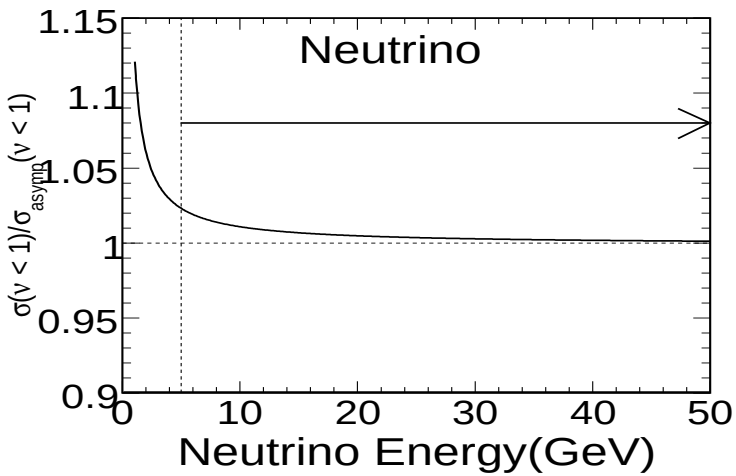

Cross Section

1. CC event sample corrected for acceptance and smearing using MC:
2. $\sigma_{\mathrm{TOT}}(E) = \frac{N_{\mathrm{xsec}}^{\mathrm{corr}}}{\Phi(E)}$
3. Correct to Isoscalar target, (Iron $\frac{N-Z}{A} = 0.0567$).

$$N_{\mathrm{xsec}}^{\mathrm{corr}}(\mathrm{E}) = N_{\mathrm{xsec}}^{\mathrm{raw}}(\mathrm{E}) \left(\frac{N^{\mathrm{MCgen}}(\mathrm{E})}{N_{\mathrm{xsec}}^{\mathrm{MCreco}}(\mathrm{E})} \right)$$

$N^{\mathrm{MCgen}}(\mathrm{E})$ = events generated in the fi ducial volume.

$N_{\mathrm{xsec}}^{\mathrm{MCreco}}(\mathrm{E})$ = events in the MC reconstructed sample.

- Normalize in region 10-50 GeV using world average ν-Iso Fe value: $\frac{\sigma^\nu}{E} = 0.676 \pm 0.01 \ \times 10^{-38} \frac{\mathrm{cm}^2}{\mathrm{GeV}}$

Total Cross Section Energy Dependence

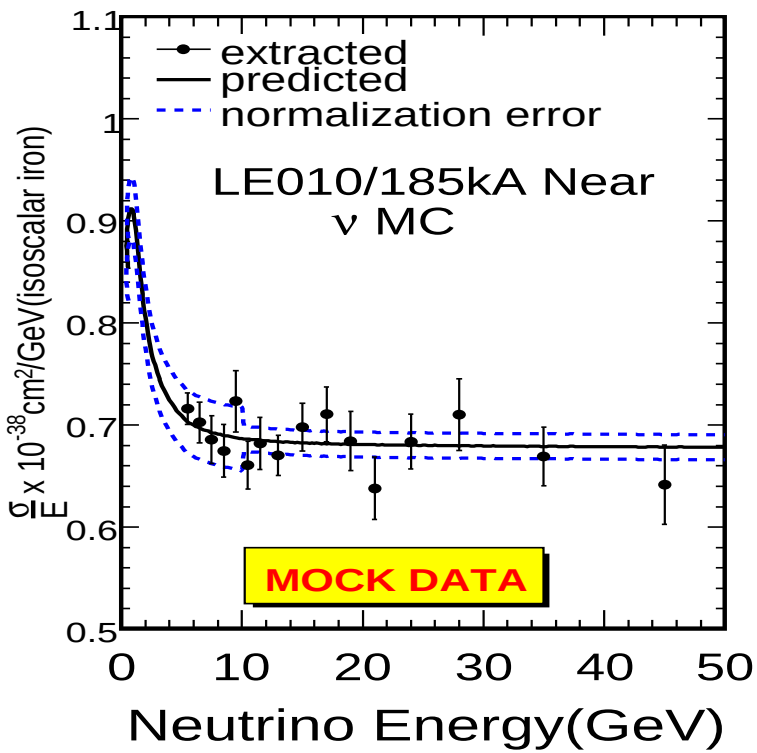

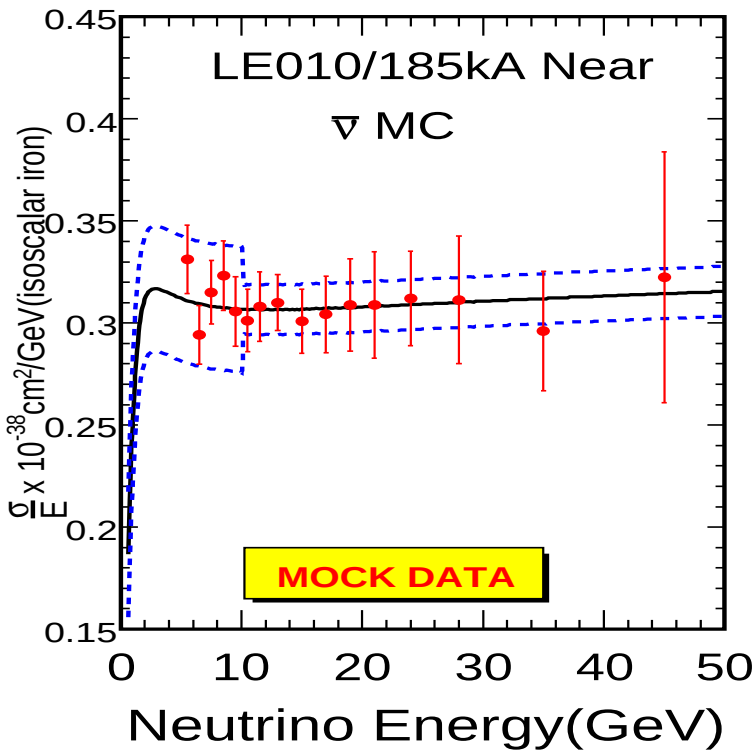

- Mock-data study, comparison to NEUGEN model prediction. (5.1$\times 10^{19}$ PoT sample).
  - Band shows size of error on the weighted average for data points with $\mathrm{E}>10\mathrm{GeV}$ (used for normalization).

Full sample (7.4$\times 10^{20}$ PoT): $\sim$15$\times$ larger
$\Rightarrow$ statistical precision $\sim$4$\times$ better.
$\Rightarrow$ Systematics will dominate.

Flux and Cross Section Errors

- Low-ν Flux method valid for $E_\nu > 5$GeV
  - At lower energies systematics from model and acceptance corrections become large.
- Expected main systematics:
  - E_μ scale $\pm$2% (Largest for Flux)
  - E_{HAD} scale $\pm$5%
  - Final state Intranuclear rescattering. (affects measured E_{HAD}) $\rightarrow$Largest for cross section,*estimate is crude, will be reduced)*.
  - Low ν sample model correction.
- Prognosis: Expect flux and cross section uncertainties in range 2-5% for $E_\nu > 5$GeV.

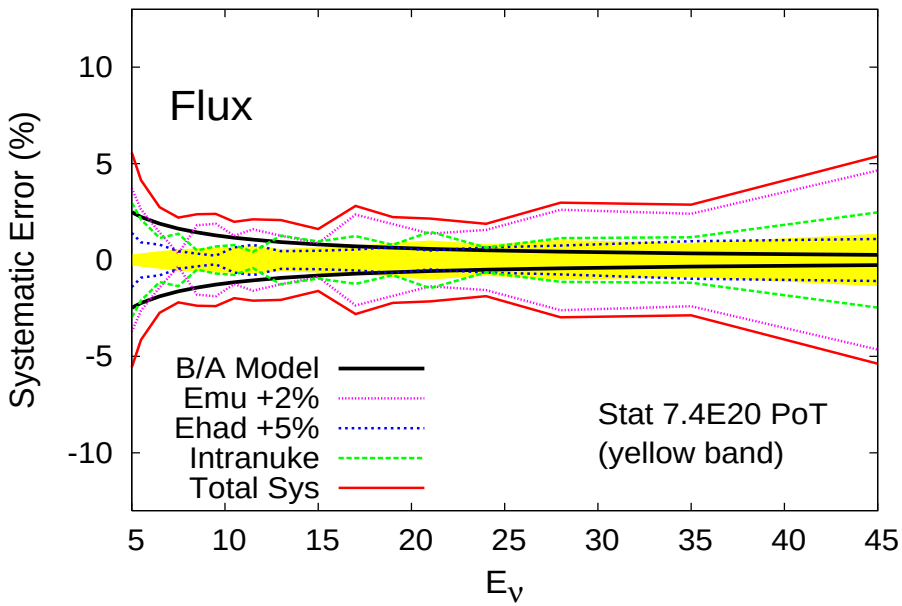

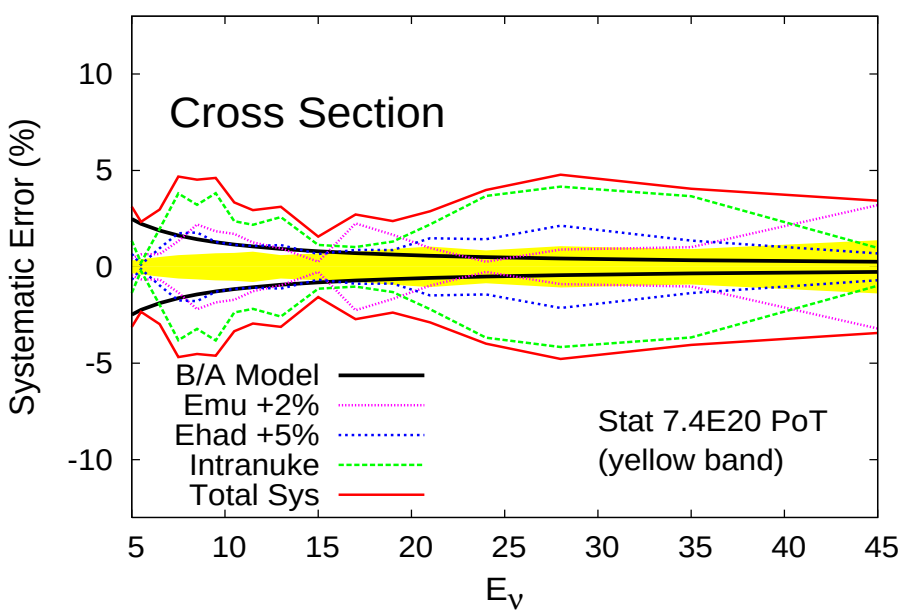

Antineutrino Sample in MINOS

- Above 5 GeV $\sim$ 15% of events are from $\overline{\nu}$.
- Total expected $\overline{\nu}$-CC sample= 7×10^5 events for 7.4E20 PoT.
- Also studying $\overline{\nu}$ flux and cross section extraction.
  - Larger model corrections to flux.
  - Acceptance corrections (μ^+s defocused).

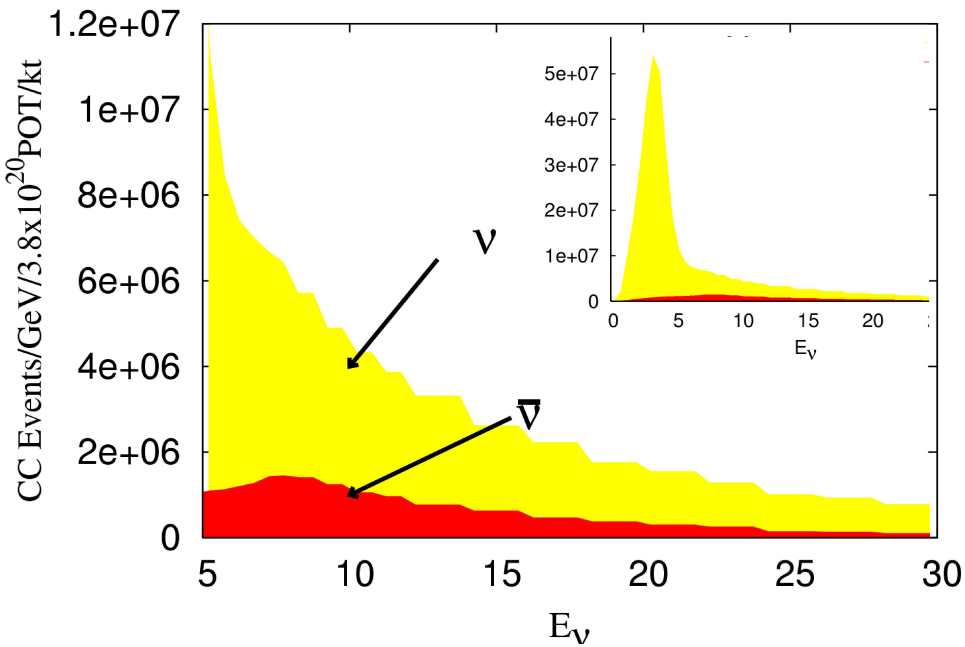

- Contamination from mis-IDed ν_μCC events is large (5-20%).
- Improvement needed to charge-sign ID to obtain high-purity sample of $\overline{\nu}$ (WIP).

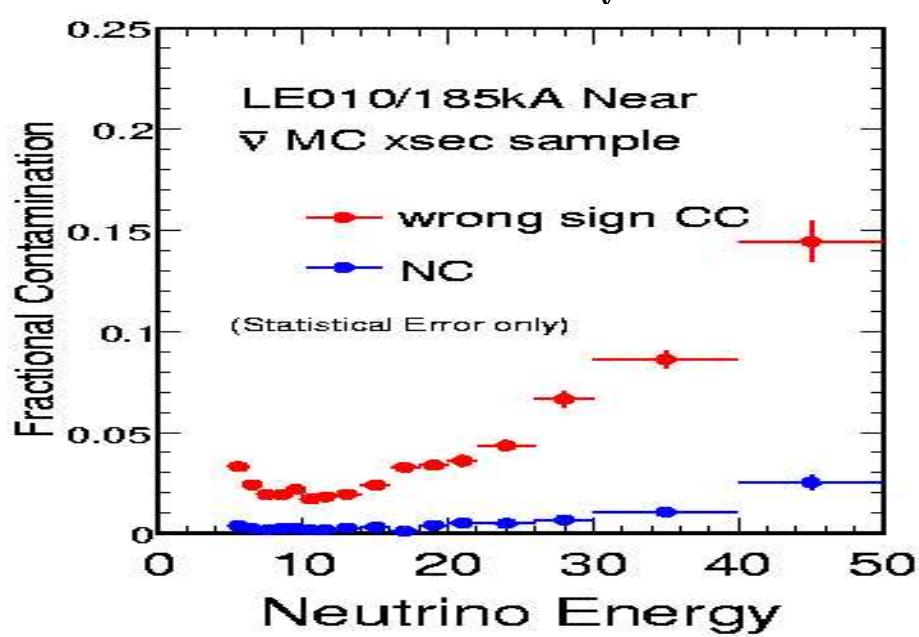

Structure Function Measurements

- Measure $F_2(x, Q^2)$ and $xF_3(x, Q^2)$ from ν and $\overline{\nu}$ differential cross sections.
- $F_2(x, Q^2)$ sensitivity - statistical errors only for 3.7$\times 10^{20}$ PoT.
  - DIS Samples: 1.3M ν, 0.2M $\overline{\nu}$.
  - Measurement uncertainty will be dominated by systematic precision.

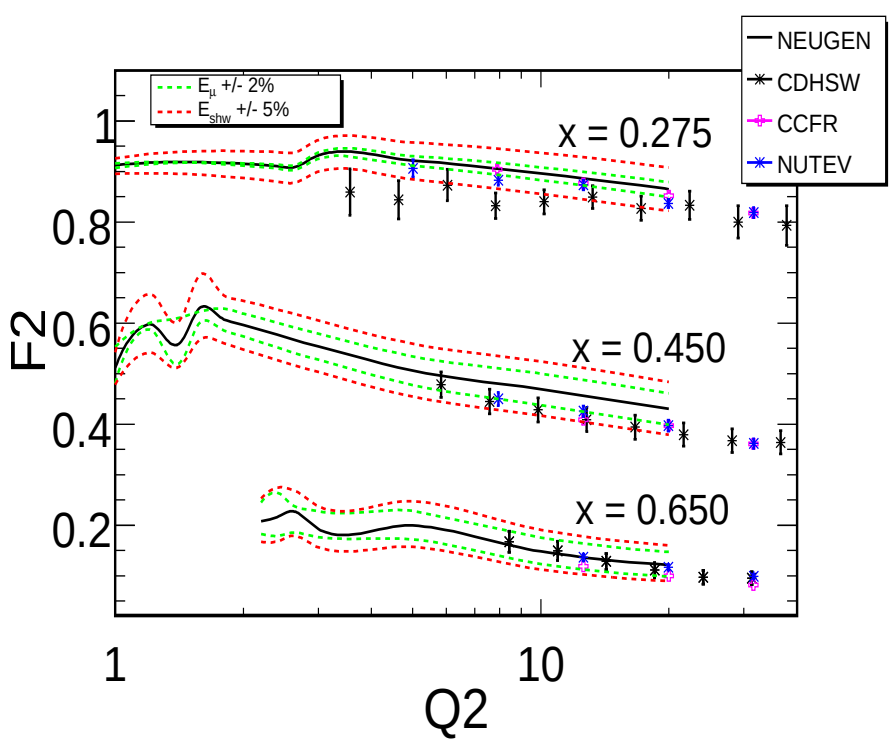

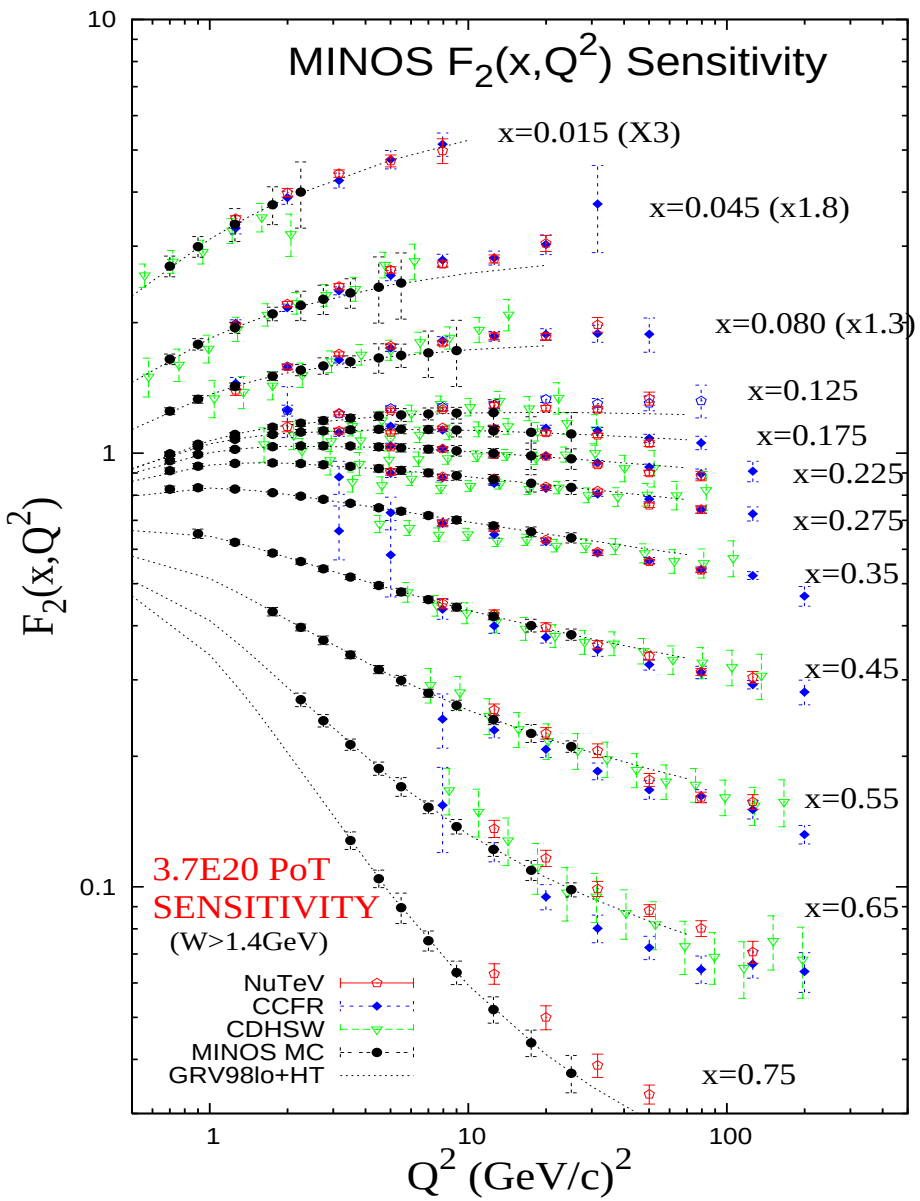

DIS with Minerνa

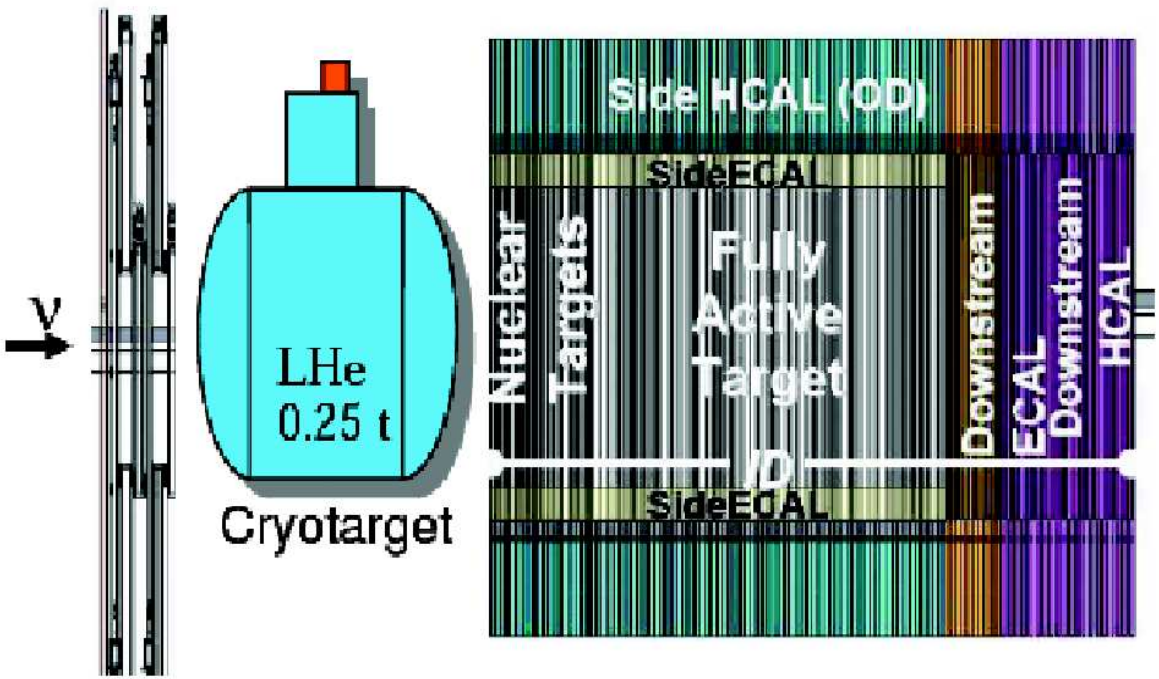

- Fine granularity
  - Fully active target (8.3t)
- Shower containment:
  - Outer layers provide Hadronic and EM calorimetry.
- MINOS ND catches muons.
  - Acceptance for DIS muons $>$90% Active TGT, $>$80% Nucl TGT

- Same kinematic range as MINOS *but with Nuclear targets!*

Nuclear targets: Pb, Fe, C, & He

Fid. masses: 0.85t Pb, 0.7t Fe, 0.2t He, 0.15t C

- Latest news: He cryotarget

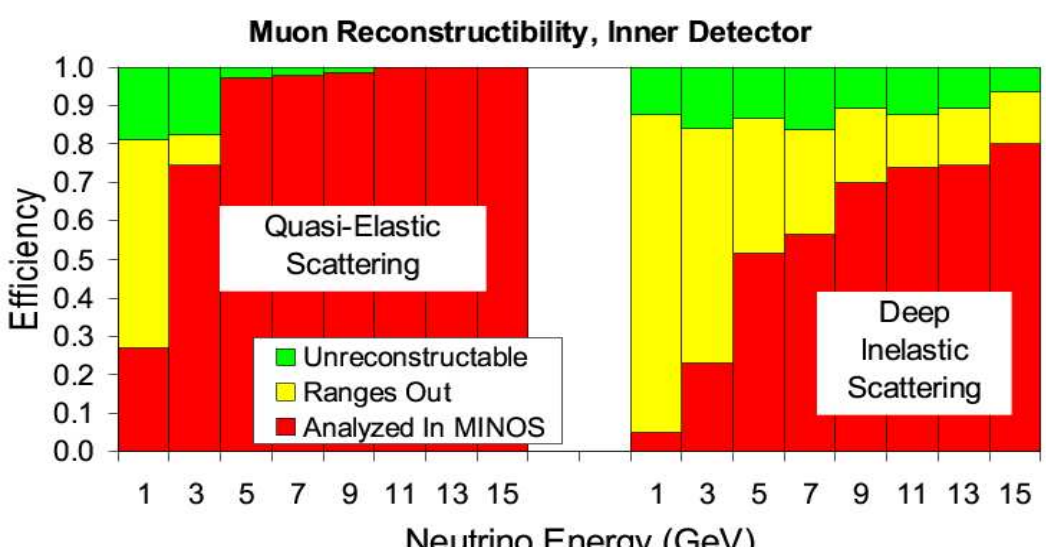

Minerνa Summary

Schedule

- Late 2007-2008 Construction of “Tracking Prototype”
  - $\sim$20% of full detector (20/108 Modules)
- Late 2008 - Minerνa Test beam detector run at FNAL M-TEST
- 2008-2009 Construction of full detector.
- Online $\longrightarrow$ 2009.

Minerνa adds to DIS arena:

- High Statistical Precision with a fine-grained detector at low energy.
  - 4 year run, 1.6×10^{21} PoT (4E20 LE/12E20 ME)
- First precise light-target (He) measurements + Heavy nuclear targets.
  - Perhaps shed light on ’EMC’-like nuclear effects in ν scattering.

DIS sample
(W$>$2 GeV, Q$>$1 GeV)

Target	Events
CH (3t)	4.3M
Pb	1.2M
Fe	1M
C	290K
He	300K

Conclusions

- Recent Results in ν-N DIS *(at High Energy)*
  - NuTeV $\star$ Precise measurement of ν-Fe differential cross sections and SF.
  - Chorus $\star$ First measurement of ν-Pb cross sections and SFs.
  - Nomad $\star$ Preliminary cross section measurements on C, Fe & Al.
- Future *(at Low Energy)*
  - Minos $\star$ Analysis underway to extract ν-Fe cross sections and SF's in low energy range (5-50GeV).
  - Minerva $\star$ Will add precise measurements on light target (He) and nuclear targets (C, Fe, Pb).

BACKUPS:*NuTeV*

Comparison with Charged Lepton Data:

apply corrections to charged lepton data:

- F_2^l/F_2^ν correction (CTEQ4D pdf):

$$F_2 = \sum_i e_i^2 q_i; \begin{cases} e_i = 1, \text{weak} \\ e_i = \frac{2}{3}\ (-\frac{1}{3}), \text{em} \end{cases}$$

$$\frac{F_2^l}{F_2^\nu} = \frac{5}{18}\left(1 - \frac{3}{5}\frac{s+\bar{s}-c-\bar{c}}{q+\bar{q}}\right)$$

- nuclear correction

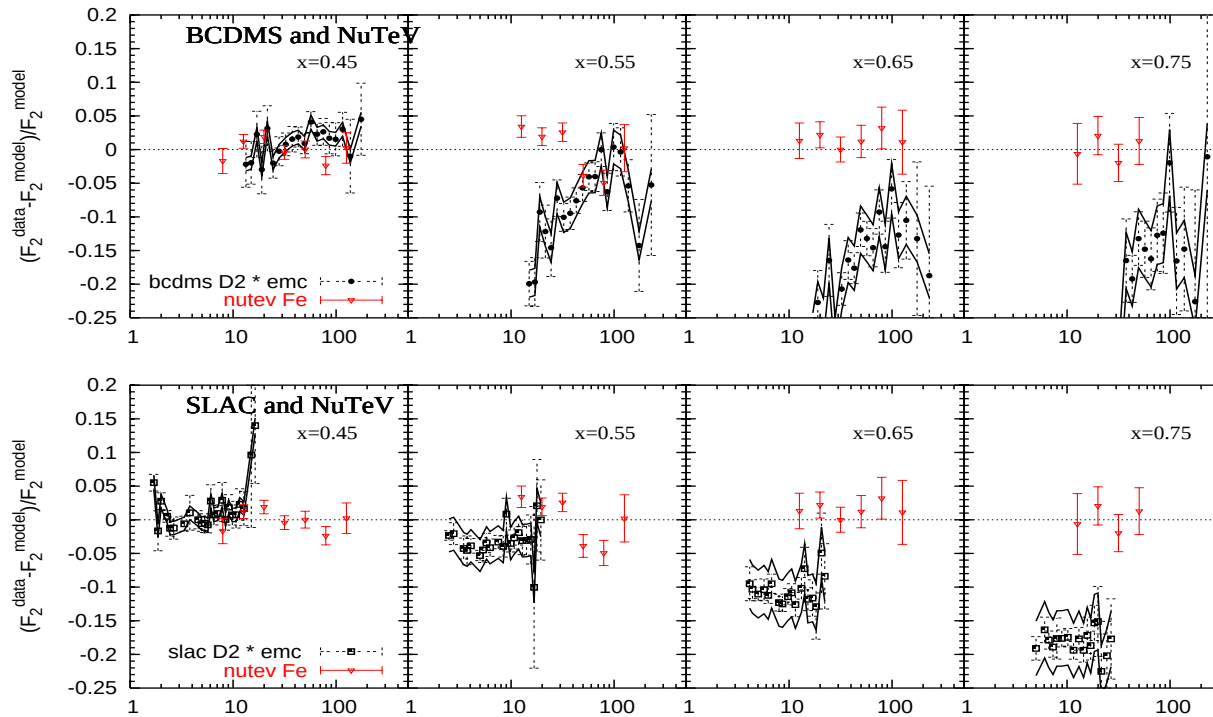

- plots show $\frac{F_2^{data} - F_{2model}^\nu}{F_{2BG}^\nu}$; data: NuTeV(Fe), BCDMS(D_2), SLAC(D_2)
- NuTeV above BCDMS(D_2) by $\approx 7\%$ at $x = 0.55$; $\approx 12\%$ at $x = 0.65$; $\approx 15\%$ at $x = 0.75$;
- NuTeV above SLAC(D_2) by $\approx 4\%$ at $x = 0.55$; $\approx 10\%$ at $x = 0.65$; $\approx 17\%$ at $x = 0.75$;

ν-scattering favors perhaps smaller nuclear effects at high x

$\Delta x F_3$ and $R(x, Q^2)$ Models

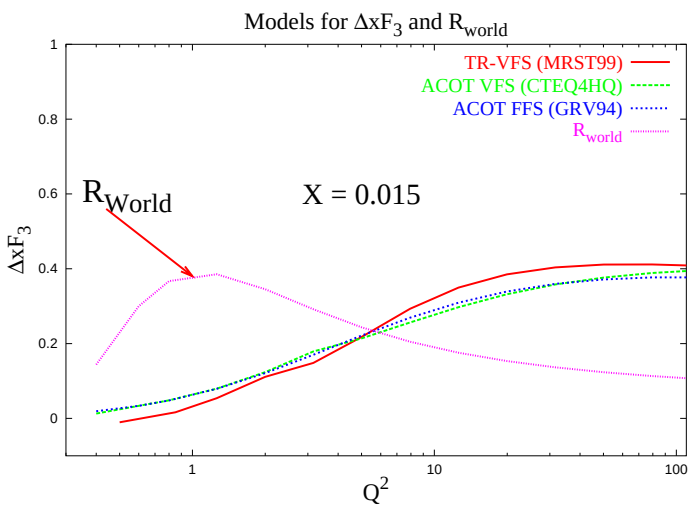

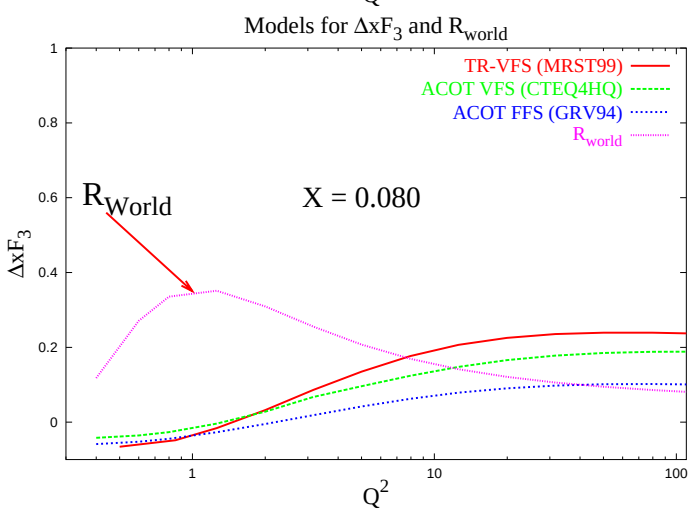

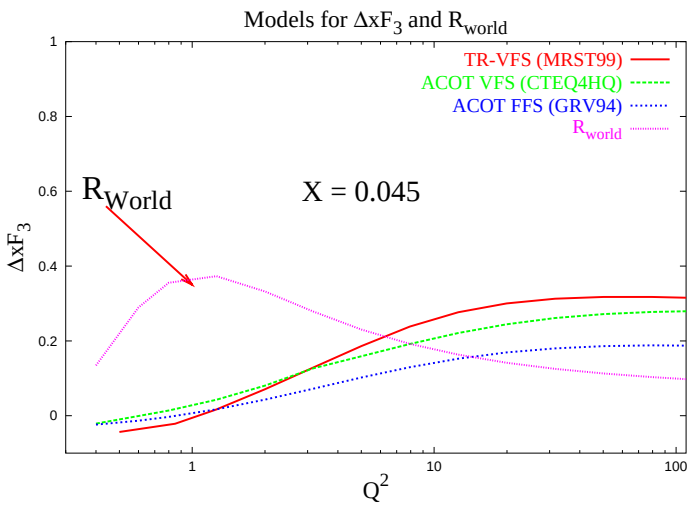

- $R_L(x, Q^2)$ [L.W.Whitlow $et.al.$ Phys.Lett. B250(1990)]
- $\Delta x F_3(x, Q^2)$ [R.Thorne and R.Roberts, Phys.Lett. B 421 (1998)]

Nuclear Correction

- correction measured in charged-lepton experiments from nuclear targets
- standard way: apply the same correct. to neutrino scattering
- we used a parametrization fit to data, independent of Q^2
  (dominated at $x > 0.4$ by SLAC)

Parametrization as function of x

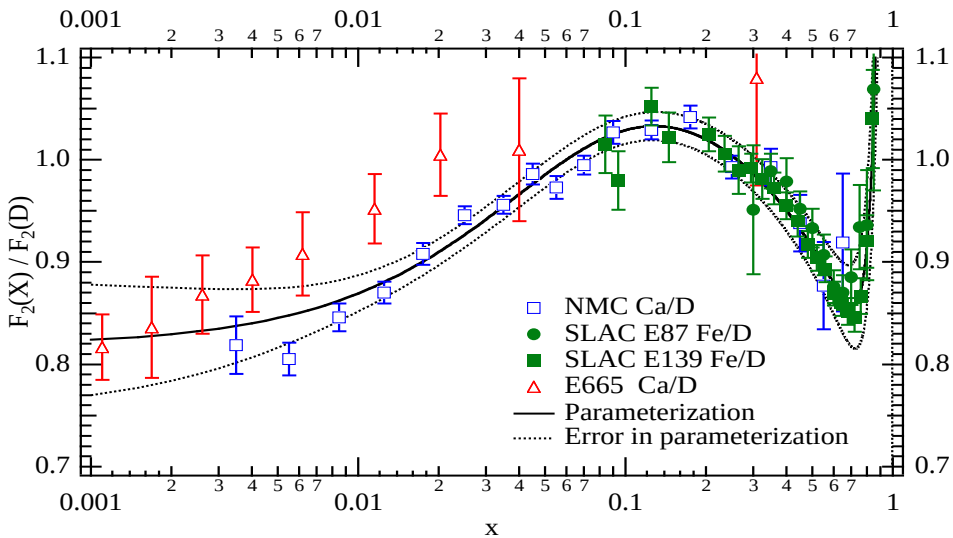

Radiative corrections

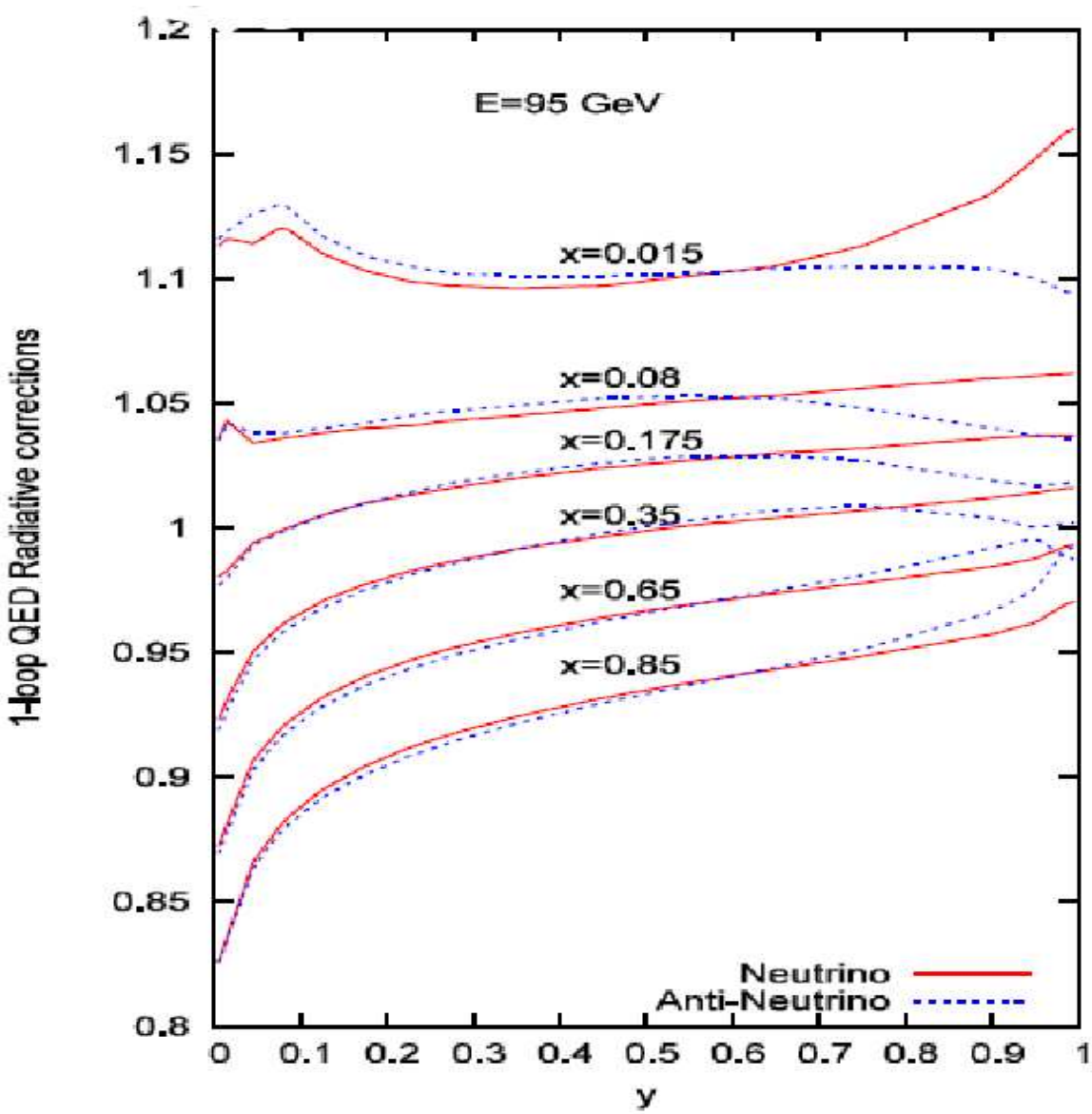

- emission of real or virtual γ by a fermion:

$$\frac{d^2\sigma}{dxdy} = \left[\frac{\left(\frac{d^2\sigma}{dxdy}\right)_{1-loop}}{\left(\frac{d^2\sigma}{dxdy}\right)_{0-loop}}\right]_{Bardin} \left(\frac{d^2\sigma}{dxdy}\right)_{Born}$$

Bardin, D. Y. and Dokuchaeva, JINR-E2-86-260 (1986)

NuTeV Cross-Section Model

- Buras-Gaemers parametrization of the valence:

$$\mathrm{xu_v(x,Q^2) = u_v^{tot}[x^{E_1}(1-x)^{E_2} + AV_2 x^{E_3}(1-x)^{E_4}]}$$
$$\mathrm{xd_v(x,Q^2) = d_v^{tot}\ xu_v(x,Q^2)\cdot(1-x)}$$
$$\mathrm{E_i = E_{i0} + E_{i1}\ln\frac{\ln Q^2/A_0^2}{\ln Q_0^2/A_0^2}}$$

- Buras-Gaemers parametrization of the sea:

$$\mathrm{x\bar{u}(x,Q^2) = x\bar{d}(x,Q^2) = \frac{1}{2(\kappa+2)}(AS(1-x)^{ES} + AS2(1-x)^{ES2})}$$
$$\mathrm{xs(x,Q^2) = x\bar{s}(x,Q^2) = \frac{k}{2(\kappa+2)}\frac{AS}{ES+1}(ES+\alpha+1)(1-x)^{ES+\alpha}}$$
$$\mathrm{AS = (ES+1)(\frac{SQ_2 - AS_2/(ES_2+1)}{SQ_3 - AS_2/(ES_2+1)(ES_2+2)}) - 2}$$
$$\mathrm{AS = (ES+1)(\frac{SQ_2 - AS_2}{ES_2+1})}$$
$$\mathrm{AS_2 = AS_{20} + AS_{21}\ln(Q^2)}$$
$$\mathrm{ES_2 = ES_{20} + ES_{21}\ln(Q^2)}$$

- Exponents ($\mathrm{E_i}$ and $\mathrm{ES_i}$) and normalization terms ($\mathrm{AV_i}$ and $\mathrm{AS_i}$) are fi tted to NuTeV differential cross-section data every loop of iteration.
- for low $\mathrm{Q^2} < 1.35\mathrm{GeV^2}$ assume GRV evolution
- assume $m_c = 1.4GeV$,$\mathrm{R_L = R_{WORLD}}$
- Higher-Twist parametrization:
  - $\mathrm{x' = x\frac{Q^2+B}{Q^2+Ax}}$

Higher Twist Effects

- Fit to ep, ed data (SLAC,BCDMS) to parameterize Target Mass and Higher Twist effects in parton-level cross section model important at high x and low Q^2.
  [hep-ex/0203009 May 2002 A.Bodek and U.K.Yang]
  - At high x and low Q^2 have to take into account the nucleon mass $\longrightarrow$ redefine x including these corrections which come as 1/Q^2 term (Target Mass effect)
  - At low Q^2 the lepton-nucleon scattering involves a double parton scattering. The contributions from HT diagrams are supressed by powers of 1/Q^2 as compared to the leading twist diagrams.

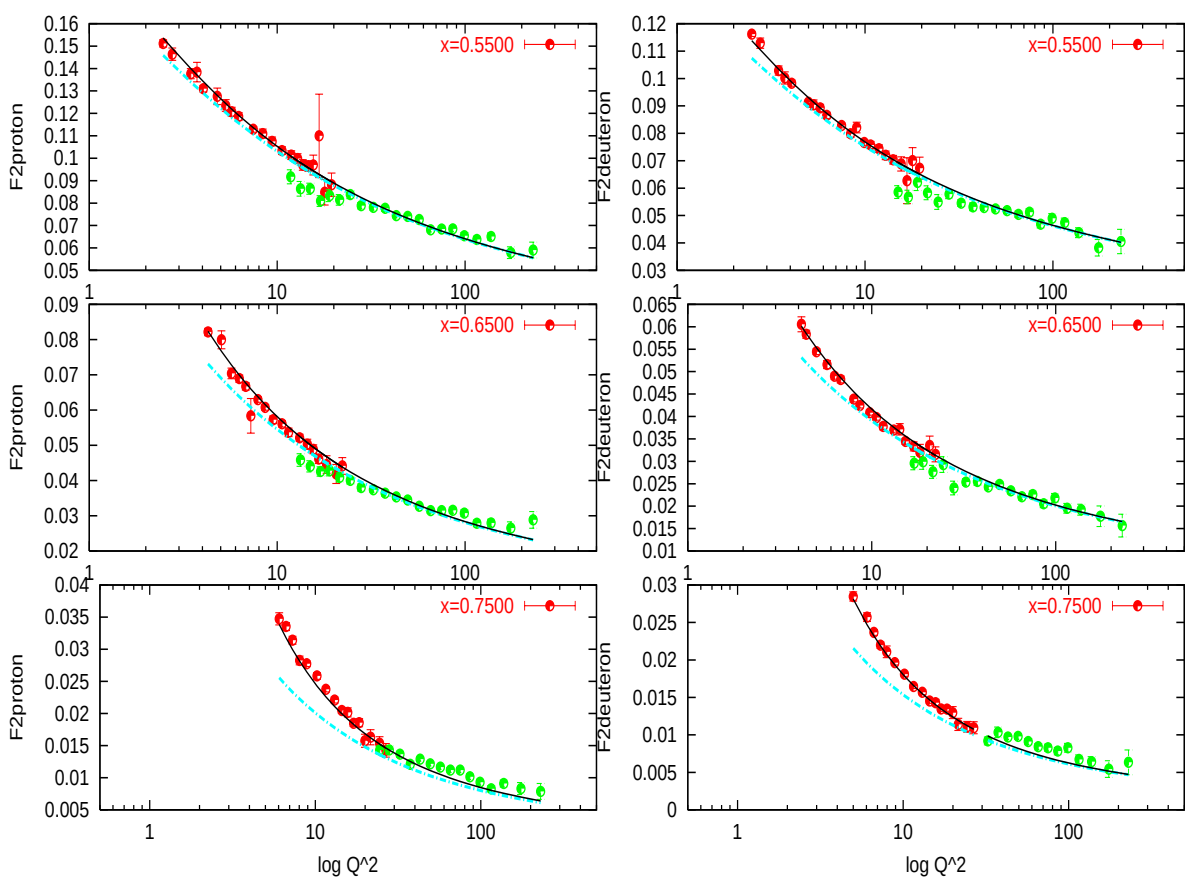

$$x' = x\frac{Q^2+B}{Q^2+Ax}$$

$$F_2 \longrightarrow \left(\frac{Q^2}{Q^2+C}\right)F_2(x', Q^2)$$

A	0.57
B	0.22
C	0.06
χ^2/dof	792/312

xF_3 Comparison with Theory Models

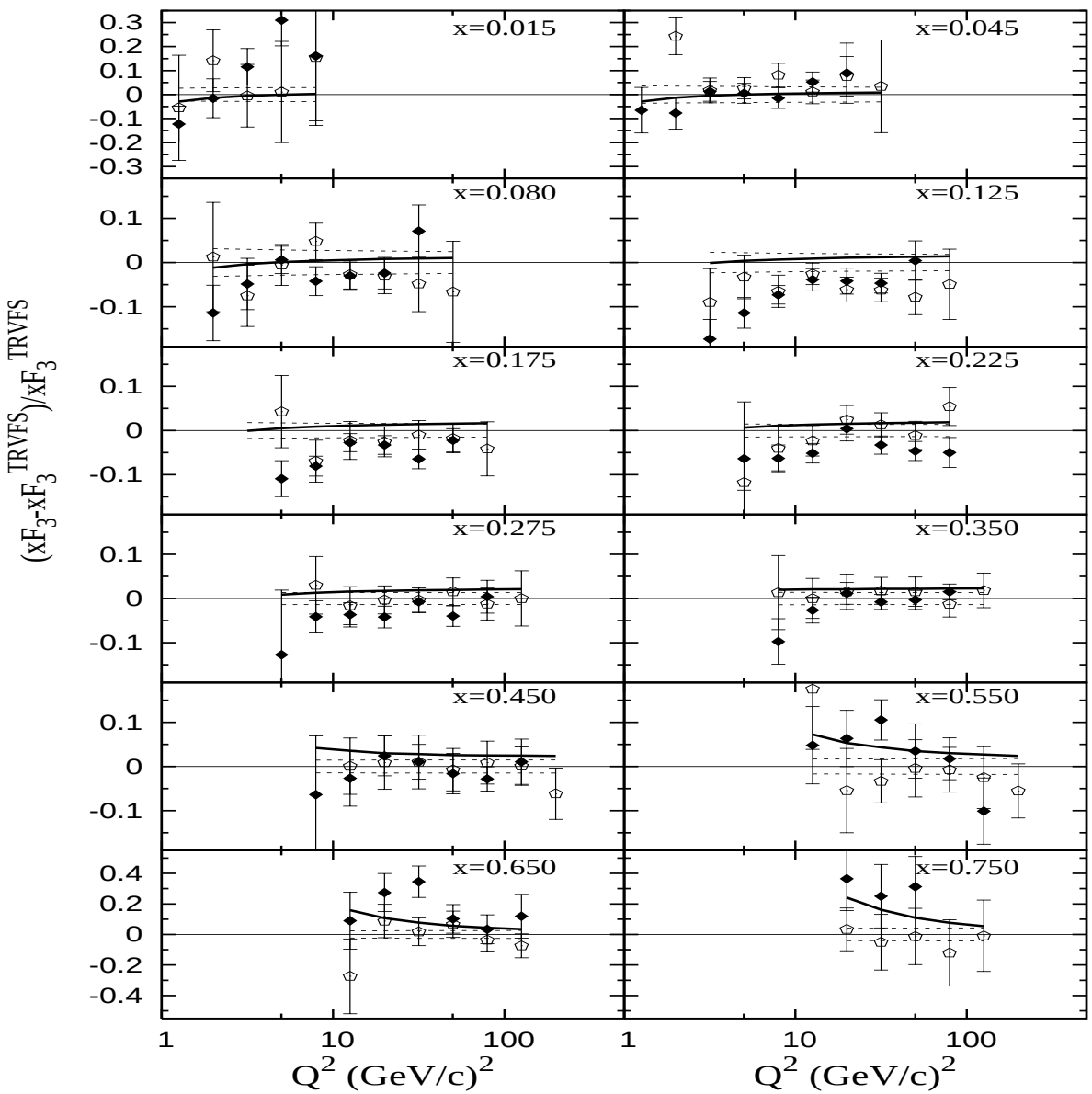

Magnetic Field NuTeV vs. CCFR

NuTeV

- ANSYS simulation, detailed geometry (incl. crack).
- Test beam 50 GeV muon map points

NuTeV Toroid Map points

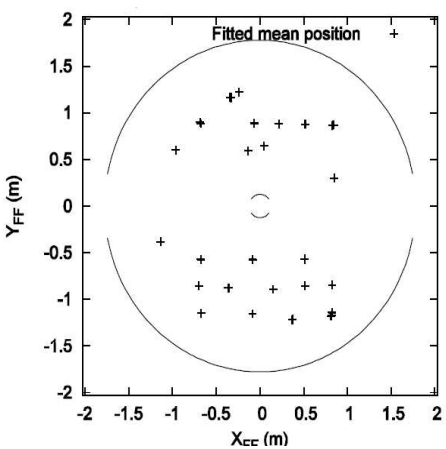

CCFR

- POISSON simulation, idealized geometry.
- Scale set by one high statistics calibration point.

$$\frac{B_\phi(CCFR)}{B_\phi(NuTeV)}$$

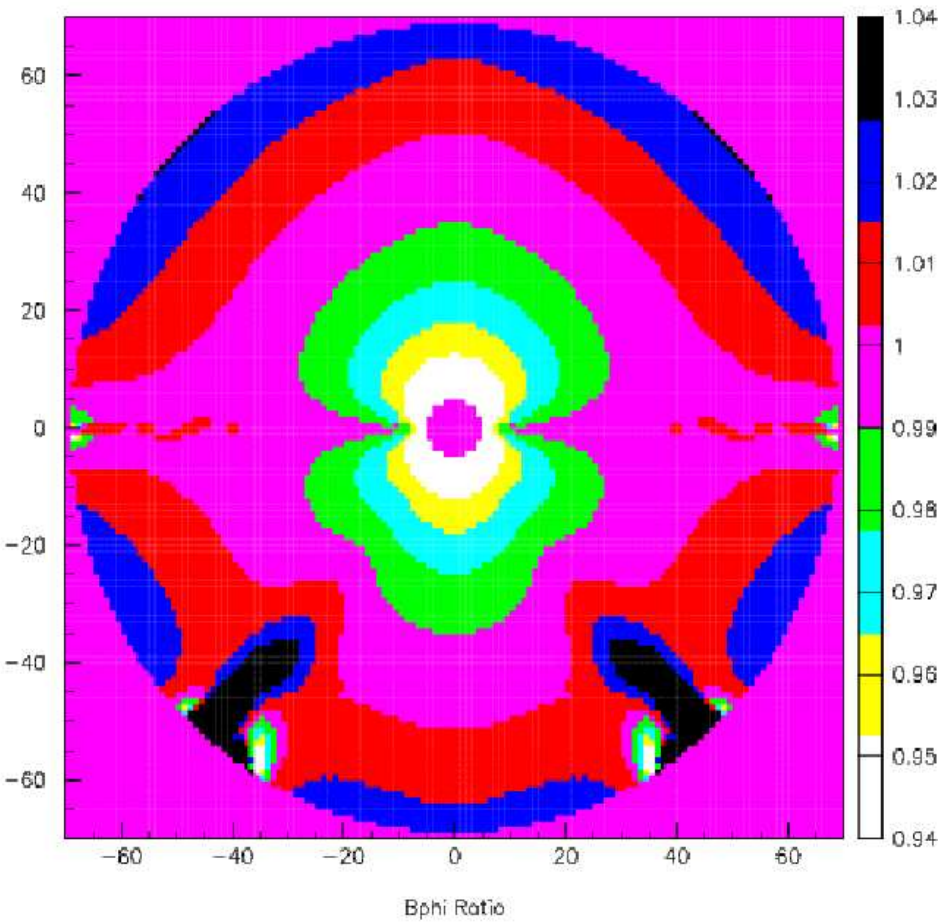

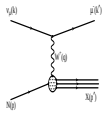

$\frac{B}{A}$ vs ν

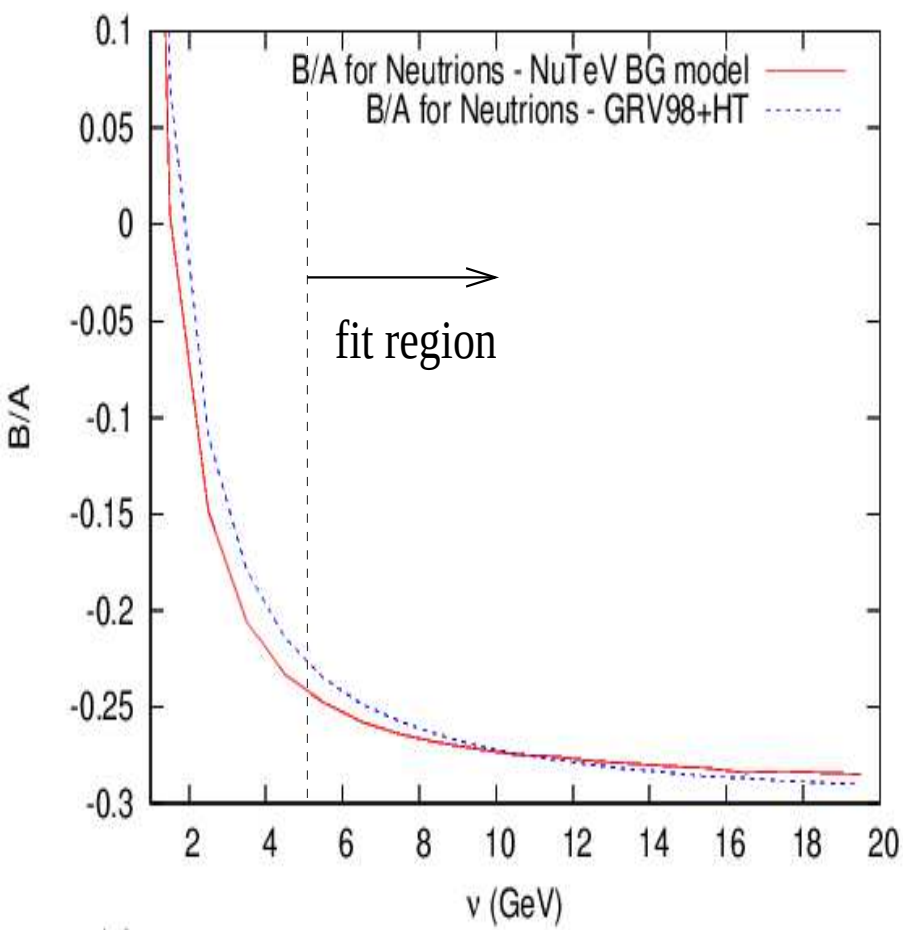
B/A for Neutrions - NuTeV BG model
B/A for Neutrions - GRV98+HT
fit region
B/A
ν (GeV)
0.1
0.05
0
-0.05
-0.1
-0.15
-0.2
-0.25
-0.3
2
4
6
8
10
12
14
16
18
20

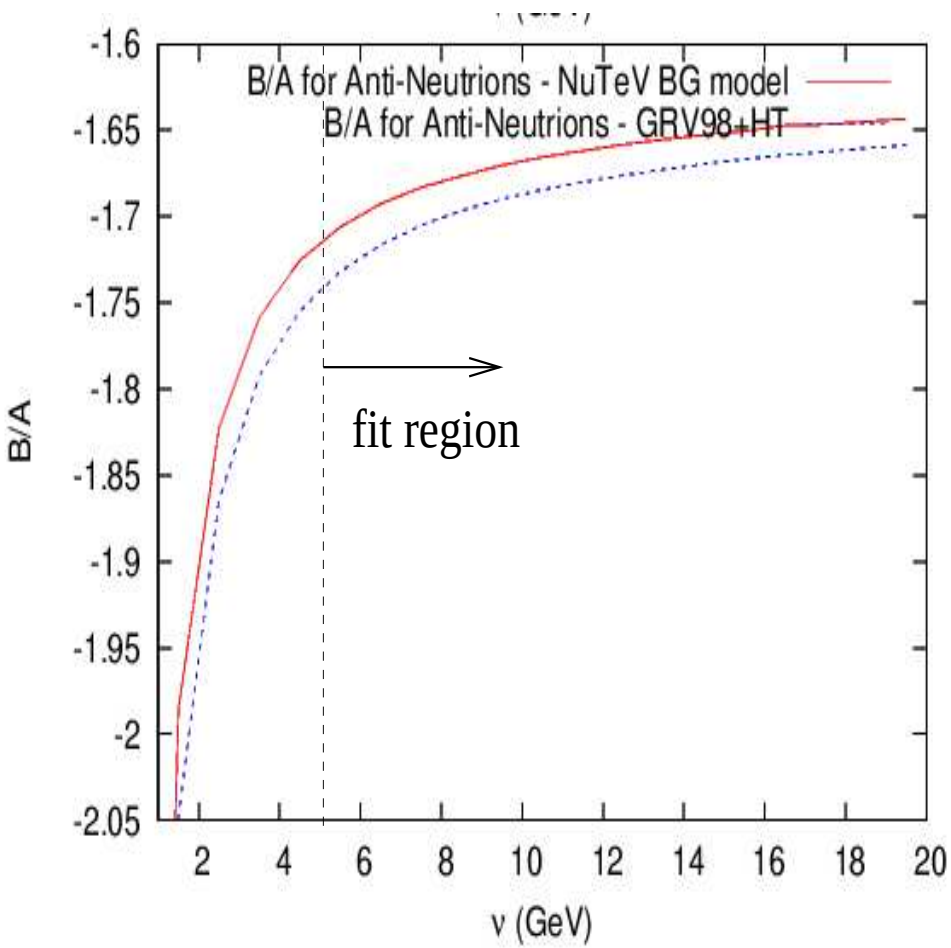
B/A for Anti-Neutrions - NuTeV BG model
B/A for Anti-Neutrions - GRV98+HT
fit region
B/A
ν (GeV)
-1.6
-1.65
-1.7
-1.75
-1.8
-1.85
-1.9
-1.95
-2
-2.05
2
4
6
8
10
12
14
16
18
20

σ/E Slope

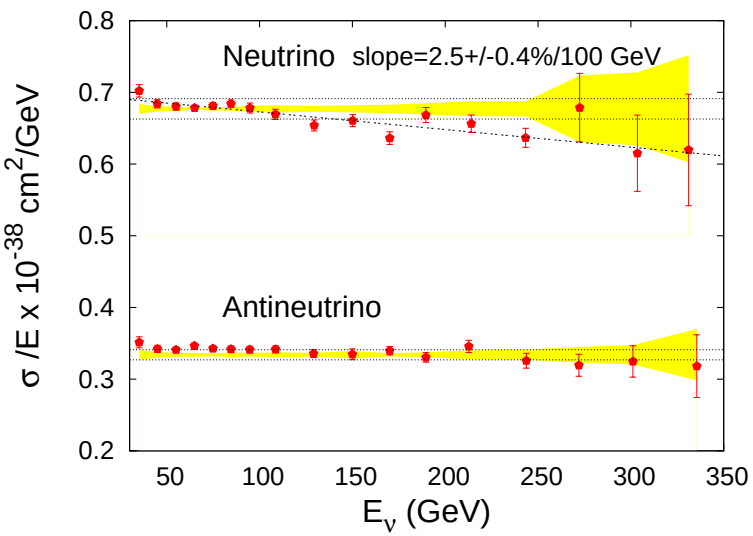

Good agreement with CCFR

$\frac{\Delta(\frac{\sigma^{\nu}}{E})}{\Delta E}$=(-2.2$\pm$0.8)% /100 GeV.

$\frac{\Delta(\frac{\sigma^{\overline{\nu}}}{E})}{\Delta E}$=(-0.2$\pm$1.3)% /100 GeV.

Extraction of Structure Functions: 2p fit

$$\frac{d^2\sigma^{\nu}}{dxdy} = \frac{2MG^2E_\nu}{\pi}\left[\left(1-y-\frac{Mxy}{2E}+\frac{1+\frac{4M^2x^2}{Q^2}}{1+R_L}\frac{y^2}{2}\right)\left(F_2^{avg}+\frac{\Delta F_2}{2}\right)+y\left(1-\frac{y}{2}\right)\left(xF_3^{avg}+\frac{\Delta xF_3}{2}\right)\right]$$

$$\frac{d^2\sigma^{\overline{\nu}}}{dxdy} = \frac{2MG^2E_\nu}{\pi}\left[\left(1-y-\frac{Mxy}{2E}+\frac{1+\frac{4M^2x^2}{Q^2}}{1+R_L}\frac{y^2}{2}\right)\left(F_2^{avg}-\frac{\Delta F_2}{2}\right)+y\left(1-\frac{y}{2}\right)\left(xF_3^{avg}-\frac{\Delta xF_3}{2}\right)\right]$$

$$xF_3^{avg}(x,Q^2) = \frac{1}{2}\left(xF_3^{\nu}(x,Q^2)+xF_3^{\overline{\nu}}(x,Q^2)\right)$$
$$F_2^{avg}(x,Q^2) = \frac{1}{2}\left(F_2^{\nu}(x,Q^2)+F_2^{\overline{\nu}}(x,Q^2)\right)$$

- Cross-Sections corrected to :
  - isoscalar target
    (5.67% excess of n over p in Fe target)
  - QED radiative effects
    [D.Y.Bardin and Dokuchaeva,JINR-E2-86-260(1986)]
- Simultaneous extraction of F_2 and xF_3 w/ input model for
  - $R_L(x,Q^2)$ [L.W.Whitlow $et.al.$ Phys.Lett. B250(1990)]
  - $\Delta xF_3(x,Q^2)$ [R.Thorne and R.Roberts, Phys.Lett. B 421 (1998)]
- Use cross section error matrix

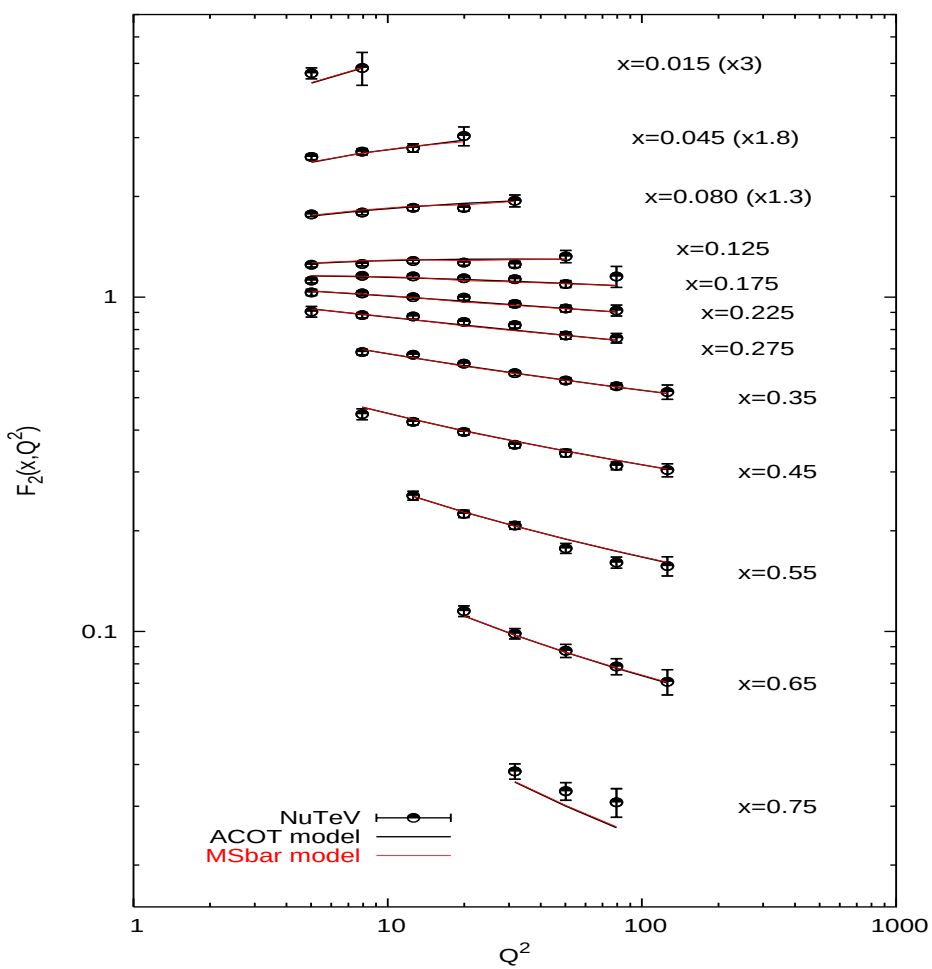

Extraction of Structure Functions: 2p fit

$$\frac{d^2\sigma^{\nu}}{dxdy} = \frac{2MG^2E_\nu}{\pi}\left[\left(1-y-\frac{Mxy}{2E}+\frac{1+\frac{4M^2x^2}{Q^2}}{1+R_L}\frac{y^2}{2}\right)\left(F_2^{avg}+\frac{\Delta F_2}{2}\right)+y\left(1-\frac{y}{2}\right)\left(xF_3^{avg}+\frac{\Delta xF_3}{2}\right)\right]$$

$$\frac{d^2\sigma^{\overline{\nu}}}{dxdy} = \frac{2MG^2E_\nu}{\pi}\left[\left(1-y-\frac{Mxy}{2E}+\frac{1+\frac{4M^2x^2}{Q^2}}{1+R_L}\frac{y^2}{2}\right)\left(F_2^{avg}-\frac{\Delta F_2}{2}\right)+y\left(1-\frac{y}{2}\right)\left(xF_3^{avg}-\frac{\Delta xF_3}{2}\right)\right]$$

$$xF_3^{avg}(x,Q^2) = \frac{1}{2}\left(xF_3^{\nu}(x,Q^2)+xF_3^{\overline{\nu}}(x,Q^2)\right)$$
$$F_2^{avg}(x,Q^2) = \frac{1}{2}\left(F_2^{\nu}(x,Q^2)+F_2^{\overline{\nu}}(x,Q^2)\right)$$

- Cross-Sections corrected to :
  - isoscalar target
    (5.67% excess of n over p in Fe target)
  - QED radiative effects
    [D.Y.Bardin and Dokuchaeva,JINR-E2-86-260(1986)]
- Simultaneous extraction of F_2 and xF_3 w/ input model for
  - $R_L(x,Q^2)$ [L.W.Whitlow $et.al.$ Phys.Lett. B250(1990)]
  - $\Delta xF_3(x,Q^2)$ [R.Thorne and R.Roberts, Phys.Lett. B 421 (1998)]
- Use cross section error matrix

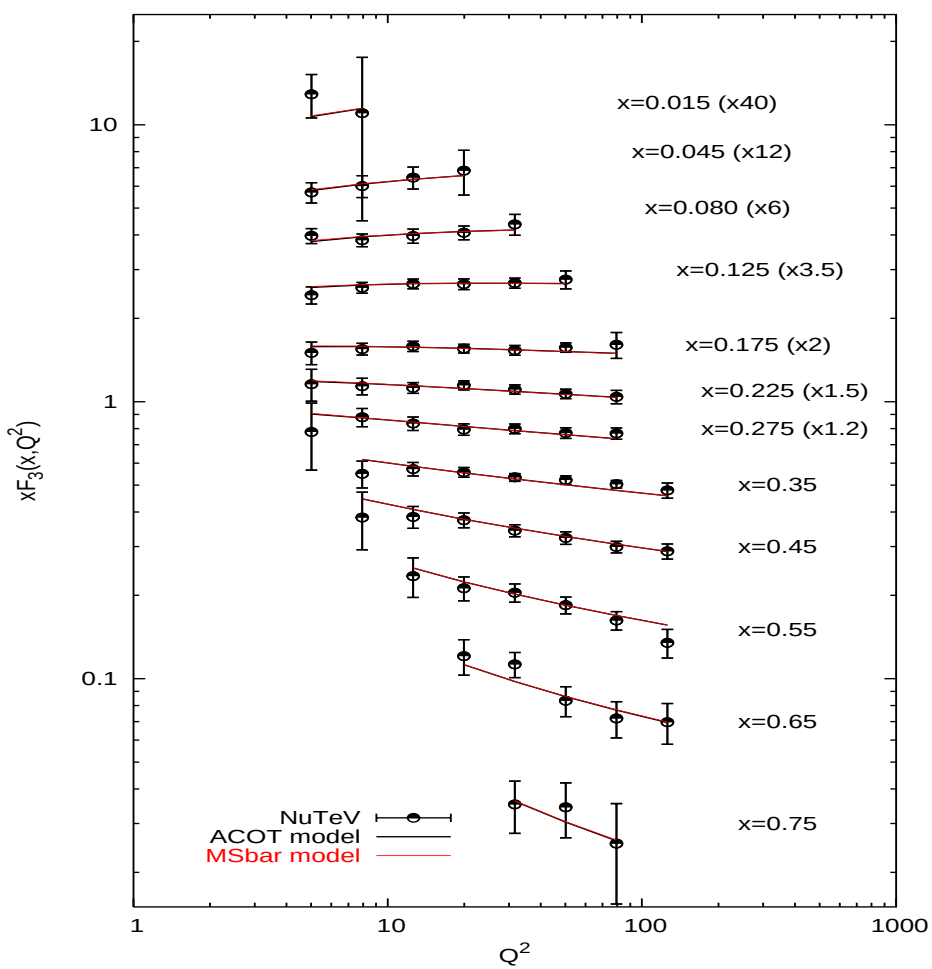

QCD Fit results

Parametrization of the PDFs at a reference scale $Q_0^2 = 5$

$$xq^{NS} = \sum_i (q_i - \overline{q_i}) = xu_v + xd_v = (A0_{u_v} + A0_{d_v}) x^{A1_{u_v}} (1-x)^{A2_{u_v}}$$

$$xq^{S} = \sum_i (q_i + \overline{q_i}) = \underbrace{xu_v + xd_v}_{xq^{NS}} + 2A0_{ud}(1-x)^{A2_{ud}}$$

$$xG = A0_g (1-x)^{A2_g}$$

- Experimental uncertainties
  - E_μ, E_{had} energy scales
  - energy smearing models
  - flux uncertainties: $\frac{B}{A}$, m_c
  - many are at the level of statistical fluctuations
- full covariance error matrix is constructed
- Theoretical Uncertainties:
  - mass quarks: negligible
  - input models: ΔxF_3, R_L
  - Scale dependence: μ_R and μ_F $\mu_F^2 = C_i Q^2$, $C_i = 1/2, 1, 2$ ($\Delta\Lambda \sim 100$MeV)

Param	xF_3 only	$F_2 + xF_3$
$\Lambda^{(n_f=4)}$(MeV)	488 $\pm$ 59	458 $\pm$ 41
$A1_{u_v}$	0.73 $\pm$ 0.01	0.72$\pm$ 0.02
$A2_{u_v}$	3.47 $\pm$ 0.06	3.49$\pm$ 0.05
$A0_{u_v} + A0_{d_v}$	4.73+2.36	4.50+2.25
$A0_{ud}$		0.67$\pm$ 0.03
$A2_{ud}$		6.83$\pm$ 0.21
$A0_g$		2.21
$A2_g$		4.30 $\pm$ 0.41
χ^2/dof	77/59	76/125
$\alpha_S(M_{Z^0})$	0.1260 $\pm$ 0.0028	0.1247 $\pm$ 0.0020

BACKUPS:*MINOS*

CC Selection Efficiency

Efficiency of $E_\mu > 2$ GeV cut.

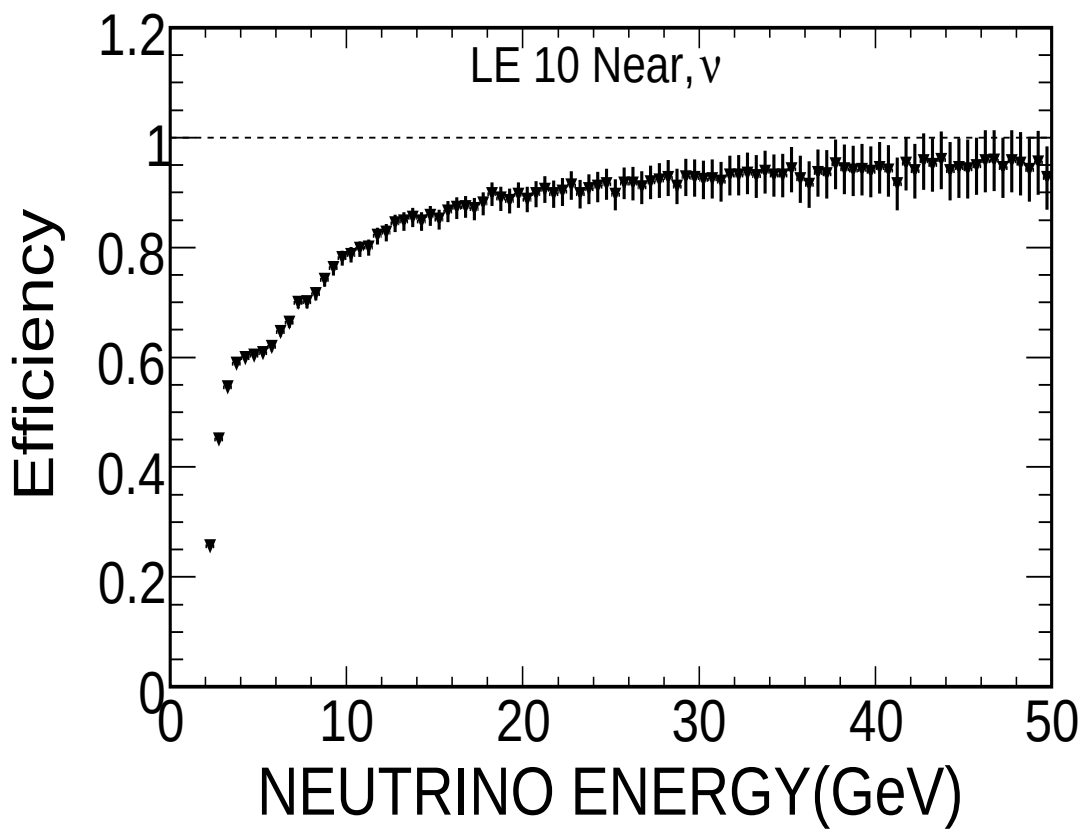

Model Corrections to Flux Extraction

Cross section model NEUGEN3 uses:

- Bodek-Yang duality model (GRV98LO pdfs tuned to data in DIS/res. overlap region.)
- QE cross section with ($M_A = 1.03$)
- No explicit contribution from resonances.
- Have also studied a NEUGEN3 version which explicitly includes resonances for $W < 1.7$) (tuned on data) and reduces the DIS contribution in the resonance region.

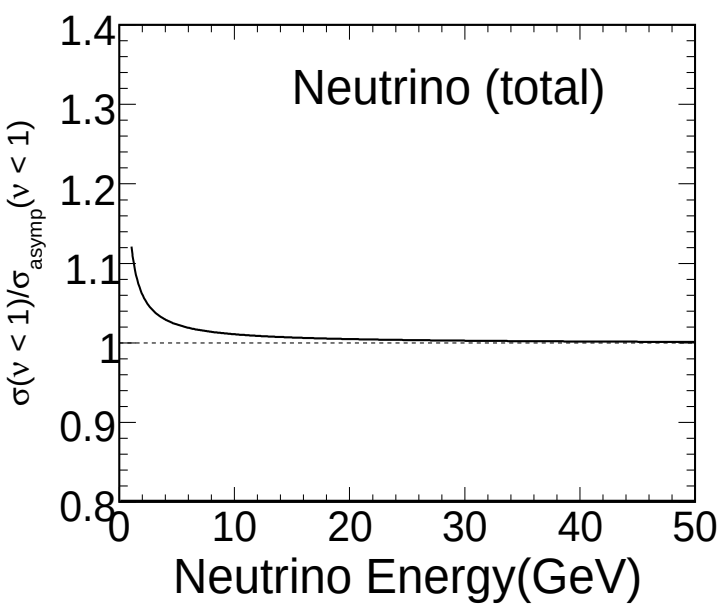

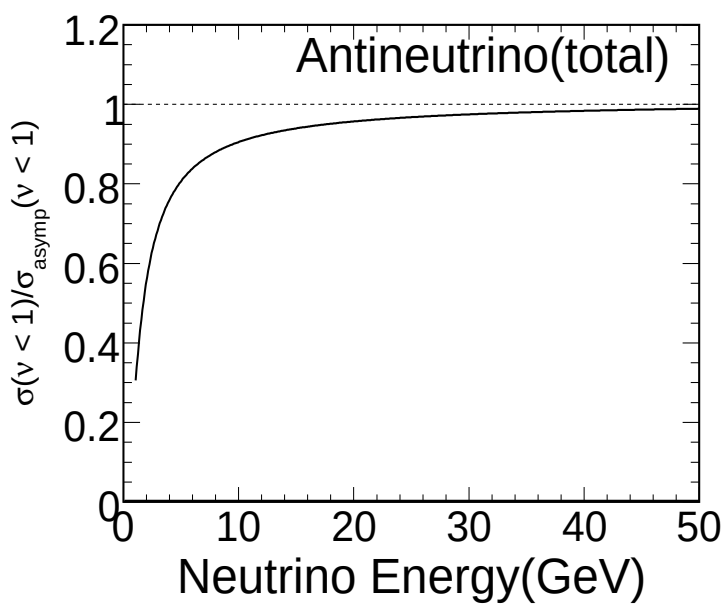

Flux Model Correction Uncertainty

Low-ν method:

$$\frac{d\sigma}{d\nu} = A\left(1 + \frac{B}{A}\frac{\nu}{E} - \frac{C}{A}\frac{\nu^2}{2E^2}\right)$$

- At low ν and high E_ν $\rightarrow$ $(\frac{\nu}{E})$ and $(\frac{\nu}{E})^2$ terms are small $\Rightarrow$ decreasing with energy.

$$\frac{B}{A} = -\frac{\int (F_2(x) \mp xF_3(x))\, dx}{\int F_2(x) dx}$$

- Smaller for ν than for $\overline{\nu}$
  - - for neutrinos: $-1 < \frac{B}{A} < 0$
  - + for anti-neutrinos: $-2 < \frac{B}{A} < -1$

- Theoretical value for $\frac{B}{A}$ computed from model, (problem: large uncertainty at low ν)
  - $(\frac{B}{A})^{\mathrm{nu}}(\nu = 20) \approx -0.25$ (lower limit)
  - $(\frac{B}{A})^{\mathrm{antinu}}(\nu = 20) \approx -1.7$ (upper limit)

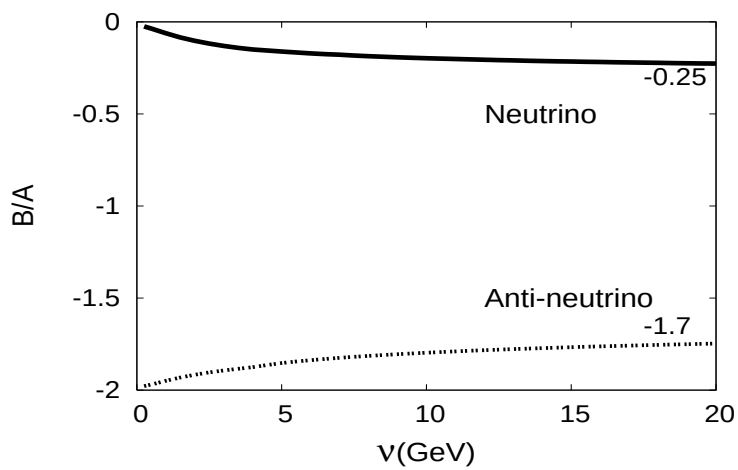

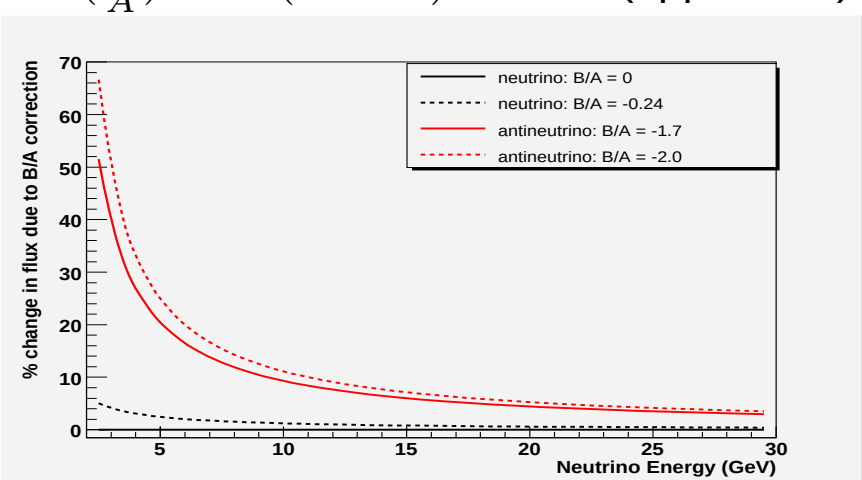

Range of DIS model uncertainty contributed by the (bounded) $\frac{B}{A}$ correction:

neutrino $\quad 0 > (\frac{B}{A})^{\nu} > -0.25$

antineutrino $-1.7 > (\frac{B}{A})^{\overline{\nu}} > -2$

Flux and Cross Section Corrections

Other physics corrections to flux and cross section

1-loop radiative corrections (Bardin), isoscalar target correction

Flux

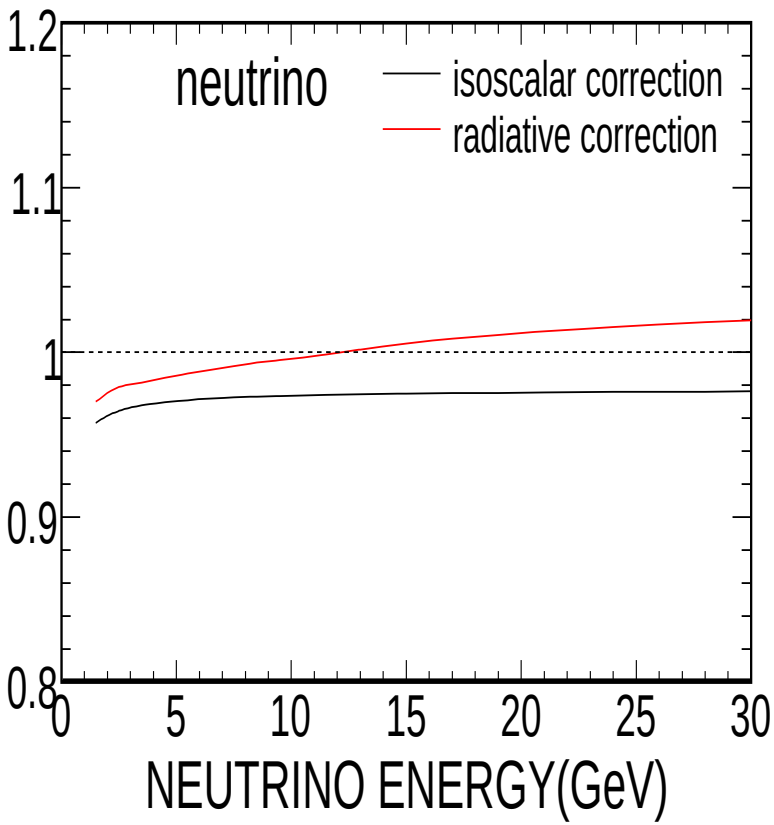

Cross Section

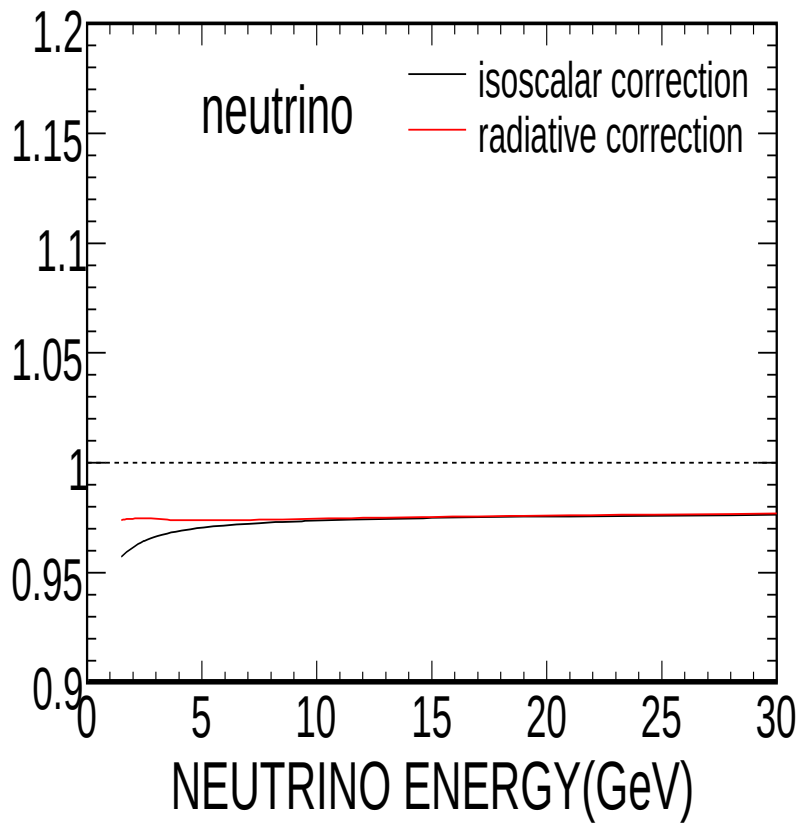

Minos Calibration System

- ▶LED based light injection system
  - Track PMT gains.
- ▶Cosmic ray muons
  - Remove variations along and between strips.
  - Stopping muons for detector-to-detector relative energy calibration.
- ▶Test beam with mini-MINOS detector (CALDET)
  - Measure absolute energy scales. (e,μ, π,p).

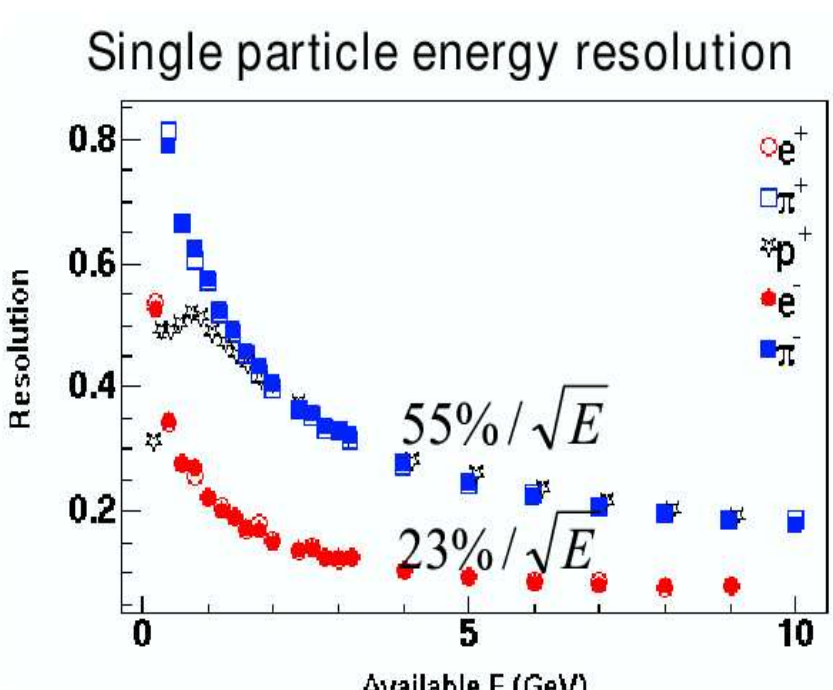

$\frac{\sigma}{E} = A \oplus \frac{B}{\sqrt{E}}$ quadratic

$\frac{\sigma}{E} = A + \frac{B}{\sqrt{E}}$ linear

Fits to the energy resolution for $\pi^{\pm}$ and p

	A (%)	B (%)	
π^+	4.2 ± 1.5	55.7 ± 0.5	quadratic
π^+	0.7 ± 0.4	55.1 ± 0.9	linear
π^-	0.0 ± 3.3	56.2 ± 0.3	quadratic
π^-	-0.1 ± 0.4	56.3 ± 0.9	linear
$\pi^+ + \pi^-$	2.1 ± 1.5	56.1 ± 0.3	quadratic
$\pi^+ + \pi^-$	0.3 ± 0.2	55.8 ± 0.4	linear
p	4.3 ± 1.4	56.6 ± 0.6	quadratic
p	0.7 ± 0.5	55.9 ± 1.0	linear

Beam Flux Errors

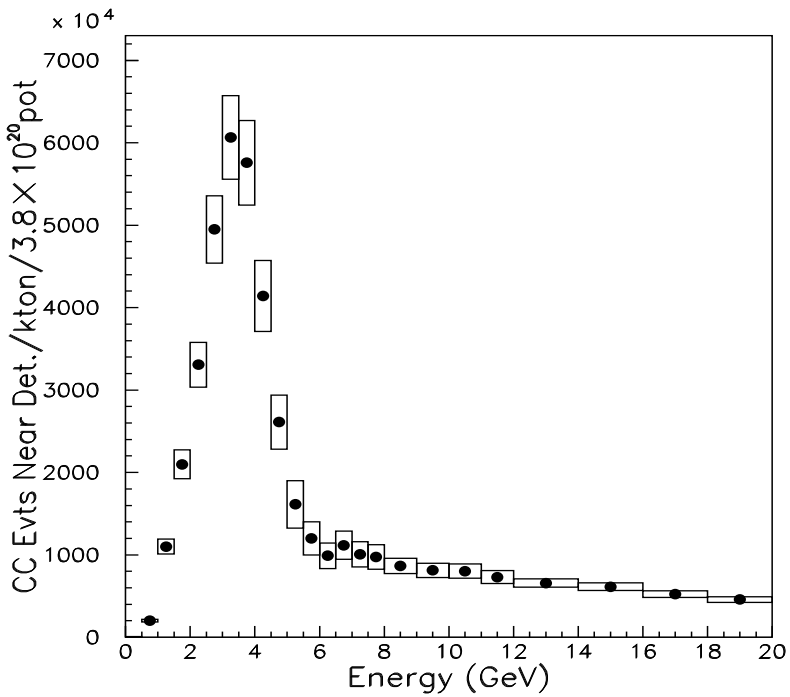

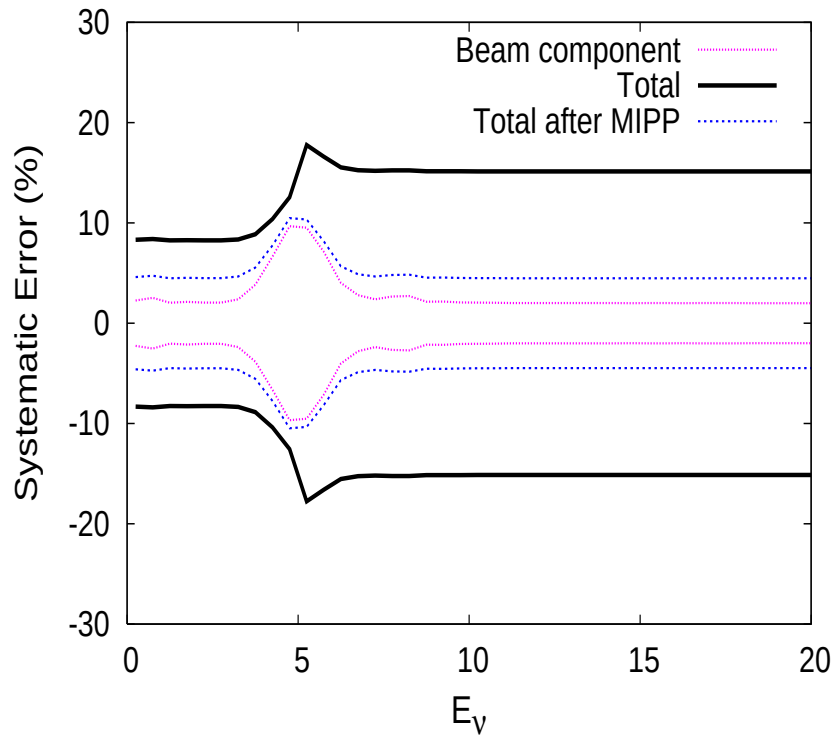

GNUMI Flux Uncertainties

- Beam component (matter most in the focusing peak region)
  1. Horn 1 offset (small)
  2. baffle scraping (small)
  3. POT (2%)
  4. Horn current offset (1%)
  5. Horn current distribution (0-8% effect)
- Production : 8-15% (15% above the beam peak).
  - Assume will be reduced after MIPP to ∼4%.

Relative Flux Extraction Method

- Use inclusive low $\nu(= E_{\mathrm{HAD}})$ cross section to get flux shape.
- *Similar method was used at higher energy (CCFR/NuTeV)$\rightarrow$ adapted to lower energies.*
- *For MINOS require $\nu < 1$GeV and extract flux for $E_\nu > 5$ GeV.*

$$\frac{\mathrm{d}^2\sigma^{\nu,\overline{\nu}}}{\mathrm{dxd}\nu} = \frac{\mathrm{G}^2\mathrm{M}}{\pi}\left[\left(1 - \frac{\nu}{\mathrm{E}} - \frac{\mathrm{Mx}\nu}{2\mathrm{E}^2} + \frac{\nu^2}{2\mathrm{E}^2}\frac{1+2\mathrm{Mx}/\nu}{1+\mathrm{R}}\right)\mathrm{F}_2(\mathrm{x}) \pm \frac{\nu}{\mathrm{E}}\left(1 - \frac{\nu}{2\mathrm{E}}\right)\mathrm{xF}_3(\mathrm{x})\right]$$

Integrate $d^2\sigma/dxd\nu$ over x for fi xed ν:

$$\frac{d\sigma}{d\nu} = A\left(1 + \frac{B}{A}\frac{\nu}{E} - \frac{C}{A}\frac{\nu^2}{2E^2}\right)$$

$$\mathrm{A} = \frac{\mathrm{G}^2\mathrm{M}}{\pi}\int \mathrm{F}_2(\mathrm{x})\mathrm{dx}$$

$$\mathrm{B} = -\frac{\mathrm{G}^2\mathrm{M}}{\pi}\int (\mathrm{F}_2(\mathrm{x}) \mp \mathrm{xF}_3(\mathrm{x}))\,\mathrm{dx}$$

$$\mathrm{C} = \mathrm{B} - \frac{\mathrm{G}^2\mathrm{M}}{\pi}\int \mathrm{F}_2(\mathrm{x})\left(\frac{1+\frac{2\mathrm{Mx}}{\nu}}{1+\mathrm{R}(\mathrm{x})} - \frac{\mathrm{Mx}}{\nu} - 1\right)\mathrm{dx}$$

- At low y, (i.e. low ν and high E_ν) $\Rightarrow$ $(\frac{\nu}{E})$ and $(\frac{\nu}{E})^2$ terms are small.

$\frac{d\sigma}{d\nu}^{\nu}_{\lim y\rightarrow 0} = \frac{d\sigma}{d\nu}^{\overline{\nu}}_{\lim y\rightarrow 0} = A$ *constant, independent of E_ν.* $\rightarrow \Phi(\mathrm{E}) \propto \mathrm{N}(\mathrm{E}, \nu < \nu_{\mathrm{o}})$.

1. Count events at low ν, $\mathrm{N}(\mathrm{E}, \nu < 1\mathrm{GeV})$
2. Use cross section model to correct for energy dependence in low-ν sample, $c(\mathrm{E}) = \frac{\sigma_{asym}(\nu<1))}{\sigma(\nu<1)}$
3. $\Phi(\mathrm{E}) \propto c(\mathrm{E})\mathrm{N}(\mathrm{E}, \nu < 1\mathrm{GeV})$

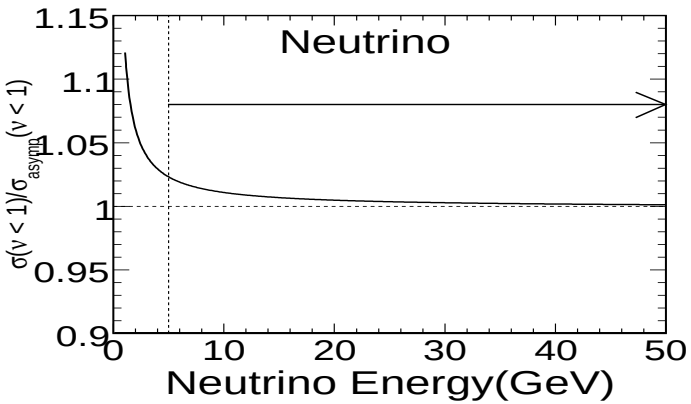

MINOS Near Detector

Magnetized tracking calormeter

- 1cm thick planes of scintillator (4.1cm wide strips).
- Sampling every 2.54cm steel.
  - Coarser → every 5 planes, in spectrometer.
- Magnetized $\langle B \rangle = 1.2\mathrm{T}$

$E_\nu = E_{HAD} + E_\mu$

Shower energy: $55\%/\sqrt{E}$
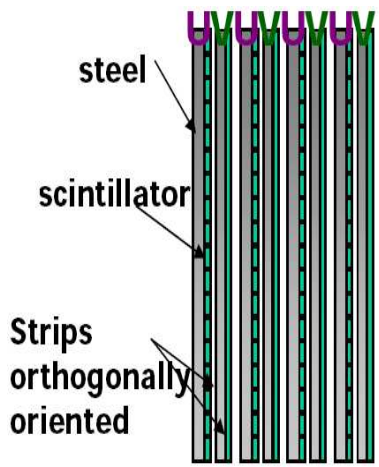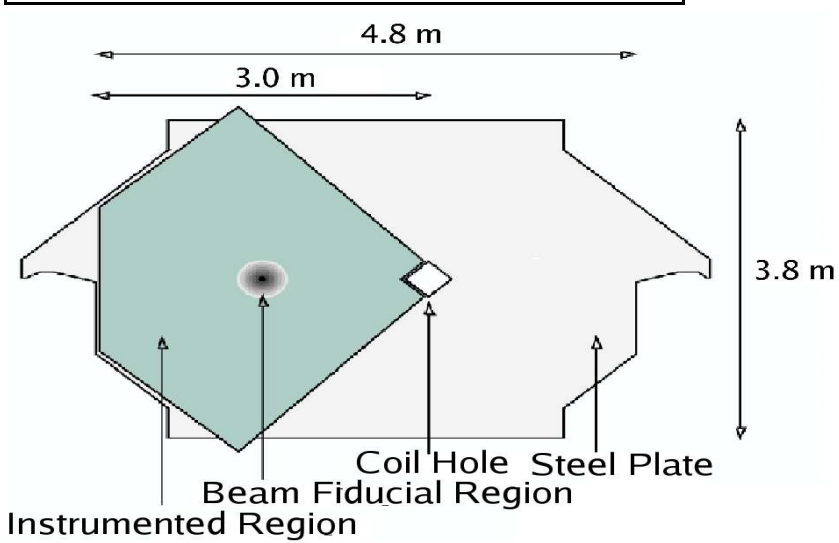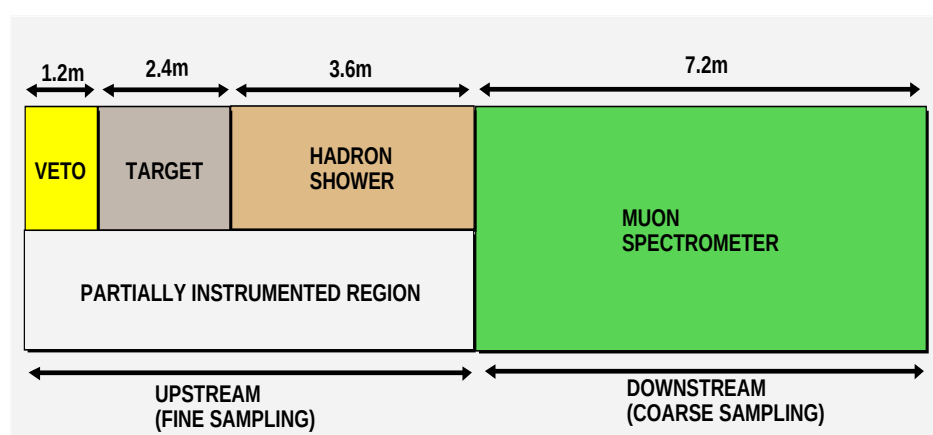
Muon energy: 6% range,13% fi t